

PETROLOGY, GEOCHEMISTRY AND ENVIRONMENTAL SIGNIFICANCE OF SILCRETE-CALCRETE INTERGRADE DURICRUSTS AT KANG PAN AND TSWAANE, CENTRAL KALAHARI, BOTSWANA

DAVID J. NASH,¹* SUE J. McLAREN² AND JOHN A. WEBB³

¹ School of the Environment, University of Brighton, Lewes Road, Brighton, BN2 4GJ, UK

² Department of Geography, University of Leicester, University Road, Leicester, LE1 7RH, UK

³ Department of Earth Sciences, La Trobe University, Bundoora, Victoria 3086, Australia

Received 12 January 2003; Revised 11 April 2003; Accepted 15 April 2003

ABSTRACT

Calcrete–silcrete intergrade duricrusts are an important component of the Kalahari Group sediments of central southern Africa and yet have neither been analysed systematically nor in any detail. In this study, the petrological and geochemical characteristics of suites of calcrete, silcrete and intergrade duricrusts from two fresh, relatively deep exposures at Kang Pan and Tswaane (adjacent to the Okwa Valley) in the central Kalahari, Botswana, are described. The duricrust profile at Kang Pan consists of a highly indurated crystalline non-pedogenic calcrete which has been extensively silicified by chalcedony, and, rarely, cryptocrystalline silica or microquartz. Silicification is most extensive in lower parts of the profile, where replacement is related to groundwater fluctuations, and in upper sections due to periodic flooding by ephemeral surface water. The exposure at Tswaane consists of a sequence of pale green glauconitic non-pedogenic silcrete and cal-silcrete overlain by non-pedogenic calcrete, all of which have formed within sediments situated upon granitoid-gneiss bedrock. The siliceous duricrusts are dominated by cryptocrystalline silica cements and appear to have developed through the replacement of a pre-existing non-pedogenic calcrete. These siliceous duricrusts have also been calcified at a later date during the formation of the overlying calcrete to produce a complex range of silica–carbonate cements. At both sites, the style and type of silicification present appears to be determined by the duration of wetting and the permeability of the precursor calcrete. Geochemical evidence indicates a lack of chemical weathering profile development within the granitoid–gneiss bedrock and considerable differences between the chemical signature of the bedrock and combined duricrusts from Kang and Tswaane. This suggests that bedrock made a minimal contribution in terms of silica and carbonate species to duricrust formation, and that the majority of cementing agents were non-local. It would therefore appear likely that the geomorphological context of each site had a major influence upon the development of calcrete, silcrete and intergrade duricrust cements. Copyright © 2004 John Wiley & Sons, Ltd.

KEY WORDS: silcrete; calcrete; duricrust; Kalahari; diagenesis

INTRODUCTION

Silica- and carbonate-cemented duricrusts form an important geomorphological control upon the development of many mid- to low-latitude landscapes and develop as a result of the dissolution, transport and precipitation of silica and carbonate by a range of near-surface low temperature physico-chemical processes operating within the zone of weathering. Such geochemical sediments are termed calcrete when they consist predominantly of calcium carbonate (Wright and Tucker, 1991), and silcrete when they contain >85 per cent silica by weight (Summerfield, 1983a). Whilst calcrete and silcrete commonly exist as discrete forms, they should more properly be considered as end-members of a spectrum of duricrust types. For example, calcretes often contain evidence for localized silicification and, less commonly, silcretes may be partly calcified. There are, however, a wide variety of geochemical sediments which contain a more mixed silica and calcium carbonate cement and therefore cannot be readily classified as either silcrete or calcrete *per se* under existing definitions. Nash and Shaw (1998) have proposed the term *silcrete–calcrete intergrade duricrust* to describe such materials.

* Correspondence to: D. J. Nash, School of the Environment, University of Brighton, Lewes Road, Brighton, BN2 4GJ, UK.
E-mail: d.j.nash@bton.ac.uk

Silcrete–calcrete intergrade duricrusts have been identified in a number of parts of the world, including North America (Price, 1933; Sidwell, 1943; Brown, 1956; Swineford and Franks, 1959; Aristarain, 1970; Reeves, 1970, 1976; Hay and Wiggins, 1980; Chadwick *et al.*, 1987; Vaniman *et al.*, 1994), South America (King, 1967), North Africa (Smith and Whalley, 1982; Thiry and Ben Brahim, 1990, 1997) and Australia (Arakel, 1986; Arakel *et al.*, 1989). However, one of the most important areas of occurrence is southern Africa (Wright, 1978; Watts, 1980; Summerfield, 1982, 1983b,c, 1984; Shaw and de Vries, 1988; Nash *et al.*, 1994a,b; Nash and Shaw, 1998; Ringrose *et al.*, 2002), where silcretes, calcretes and intergrade duricrust varieties form a major component of the Kalahari Group sediments (South African Committee for Stratigraphy, 1980). Three main silcrete–calcrete intergrade types have been identified in this region on the basis of silica–carbonate associations within the duricrust cement (Nash and Shaw, 1998). These are (a) duricrusts where extensive secondary silicification has occurred within a calcareous matrix; (b) varieties where secondary carbonate has been precipitated within a siliceous matrix; and (c) materials where silica and carbonate matrix cements appear to have been precipitated either contemporaneously or in close succession. Further sub-types have been identified within each of these three groups, dependent upon whether secondary materials have either replaced pre-existing cements or have simply been precipitated in pore spaces and voids within a pre-existing geochemical sediment.

To date, much of the research on silcrete–calcrete intergrade crusts in the Kalahari has been limited to the analysis of small outcrops or grab samples. This is mainly due to the flat topography and relatively limited landscape incision in the region, restricting the opportunities for exposure of sub-surface crusts. Where extensive outcrops of silcrete or calcrete are present, such as in the flanks of dry valley systems or around ephemeral lakes and pans (Mallick *et al.*, 1981; Shaw and de Vries, 1988; Nash *et al.*, 1994a,b; Ringrose *et al.*, 2002; Nash and McLaren, 2003), the exposures have been invariably subject to long periods of weathering and chemical alteration, making the interpretation of cement interrelationships problematic. However, the excavation of aggregate quarries during the construction of the Trans-Kalahari Highway in the mid- to late 1990s created a number of large, deep pits which provide access to relatively unweathered exposures of Kalahari Group sediments. The majority of these pits expose pedogenic and non-pedogenic calcrete (Nash and McLaren, 2003), but two sites in the central Kalahari, Botswana (Figure 1), reveal unusually thick sequences of silcrete–calcrete intergrade duricrusts. The first of these locations is a pit excavated into the floor of Kang Pan, revealing 5.5 m of Kalahari Group intergrade duricrusts. The second is a quarry on the flanks of the Okwa Valley at Tswaane, in which a 9 m thick sequence of duricrusts and underlying Precambrian bedrock is exposed.

The aim of this paper is to present the first in-depth investigation of cement relationships within Kalahari silcrete–calcrete intergrade duricrusts at a profile scale, through the detailed analysis of the petrology and geochemistry of duricrusts and bedrock exposed within the quarries at Kang and Tswaane. These sites offer a rare opportunity to study silica–carbonate relationships within thick, unweathered, intergrade duricrusts and allow the processes by which such complex geochemical sediments developed to be identified. The differences between the two sites in terms of their geological and geomorphological contexts also allow the potential influence of host materials and landscape setting upon duricrust development to be assessed. From these investigations, the wider environmental implications of the processes of geochemical sedimentation are discussed. Despite their relatively widespread occurrence, these types of complex duricrust are poorly understood; as such, this study represents an initial attempt at characterization.

Throughout the paper, calcretes, silcretes and intergrade forms such as sil-calcrete and cal-silcrete are distinguished using the criteria set out by Nash and Shaw (1998). Where the SiO₂ content of a duricrust, determined by bulk chemical analysis, exceeds 85 per cent it is termed a silcrete (after Summerfield, 1983a), and where it contains more than 50 per cent CaCO₃ by volume it is a calcrete. If bulk chemical analysis demonstrates that a sample falls into an intergrade category it is classified according to the dominant cementing agent: cal-silcrete for any duricrust in which silica dominates the cement but carbonate is also present, or sil-calcrete in a calcrete where silica is present. In the case of samples which fall close to these boundaries, point-count data of the percentage of different cement types present are used to classify the material in order to overcome the effect of host material influences upon bulk chemical composition. The terms cal-silcrete and sil-calcrete do not necessarily imply that a particular cement is primary or secondary in a stratigraphic sense. For example, cal-silcrete may refer to a calcrete with secondary silica cement but may also be applied to an extensively silicified calcrete where silica has replaced carbonate to become the dominant cement.

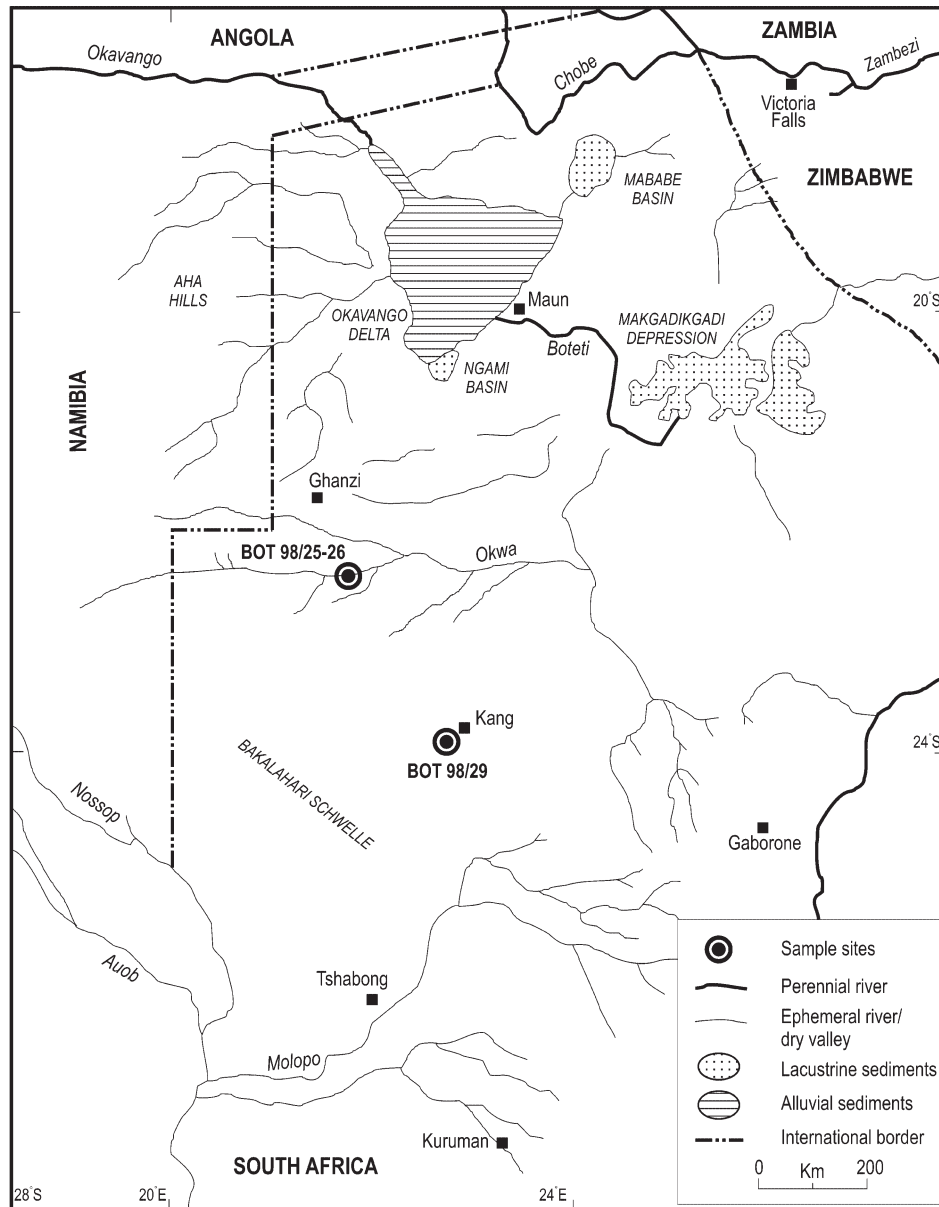


Figure 1. Locations of sample sites at Tswaane and Kang Pan

LOCATIONS OF STUDY SITES AND THEIR GEOMORPHOLOGICAL SETTINGS

The quarry at Kang Pan is located at $23^{\circ}41'44''$ S, $022^{\circ}47'51''$ E and is situated to the west of Kang village on the southern margin of the pan floor, with the aggregate pit excavated into the pan floor sediments. The quarry measures approximately 50 by 30 m and exposes a maximum of 5.5 m of duricrust grading from cal-silcrete near the base of the exposure to calcrete in upper sections of the pit (Figure 2A,B). The sequence at this site is entirely within Kalahari Group sediments with no older underlying bedrock exposed. Despite being located within the pan floor, there was no water present within the pit at the time of sampling. A single profile (BOT 98/29) was sampled at Kang Pan on the side of the quarry closest to the pan centre.

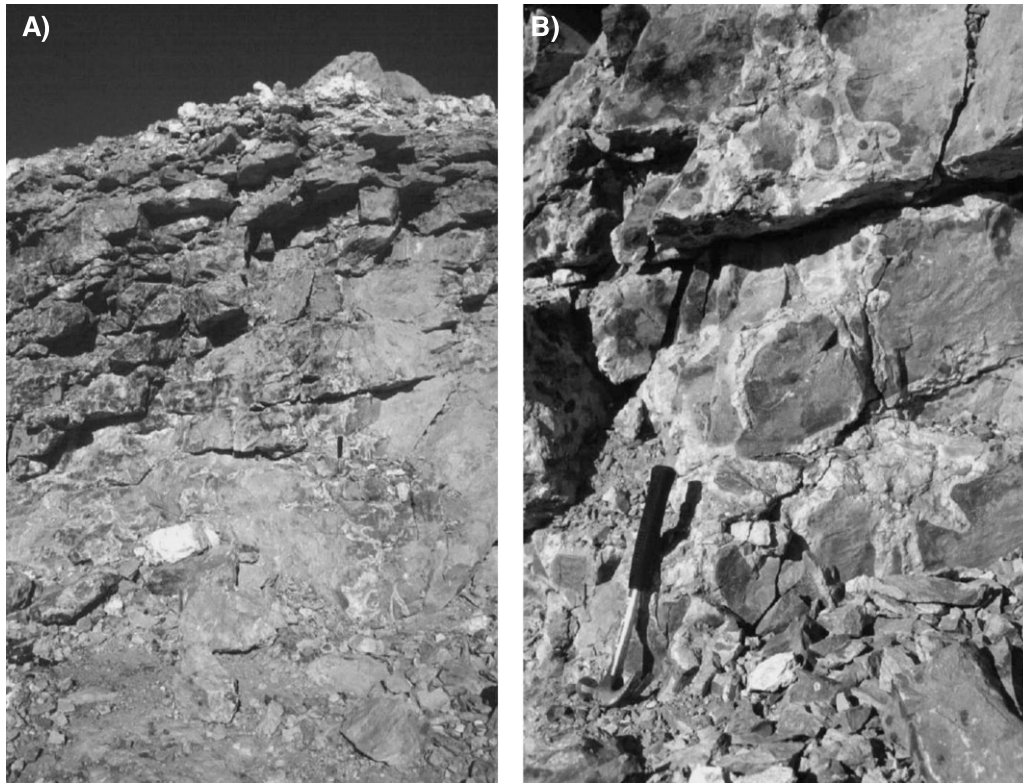


Figure 2. Views of sample Profile BOT 98/29 from Kang Pan: (A) view of the sample profile; (B) close-up of profile showing patchy silicification and alteration of pre-existing calcrete

Tswaane Quarry is located at 22°24'10" S, 021°50'34" E, approximately 2 km east of the Trans-Kalahari Highway, and is excavated through a thin cover of Kalahari Group sediments into a major inlier of Proterozoic granitoid-gneiss bedrock (Aldiss and Carney, 1992). The quarry is situated on a relatively flat plateau surface immediately south of the Okwa Valley, and very close to the weathered outcrops of calcrete and silcrete exposed in the valley flank described by Nash *et al.* (1994b). Indeed, it is likely that the duricrusts exposed within the valley flank are a continuation of those in the quarry. The quarry measures approximately 200 by 150 m (with its sides oriented broadly east–west and north–south), has a maximum depth of over 12 m near its northern edge and provides an extensive exposure of calcrete, silcrete and cal-silcrete overlying fresh and unaltered bedrock (Figure 3A,B). Water was present in the deepest part of the quarry at the time of sampling, suggesting that the base of the pit intersected the water table and may therefore be below the floor of the adjacent dry valley. Duricrust and bedrock samples were collected from two profiles on the east (profile BOT 98/25) and south (BOT 98/26) sides of the pit.

METHODOLOGY

At all three sections at Kang Pan and Tswaane Quarry, duricrust and/or bedrock exposures were logged and sampled at 50 cm intervals and the landscape context noted. This produced a total of 42 samples for further analysis. Details of sample numbers, profile thickness and general lithological characteristics are shown in Tables I–III. All samples were split prior to analysis in thin-section using a binocular microscope. Three-hundred point-counts were made per thin-section to quantify the percentage of host materials, porosity, and carbonate and silica cement types present. Host material point-counts for samples from Tswaane Quarry included an assessment of fresh and fragmented bedrock together with Kalahari Sand quartz grain content, whilst only quartz grains were present at Kang Pan. Cement counts were segregated to allow the identification of cryptocrystalline

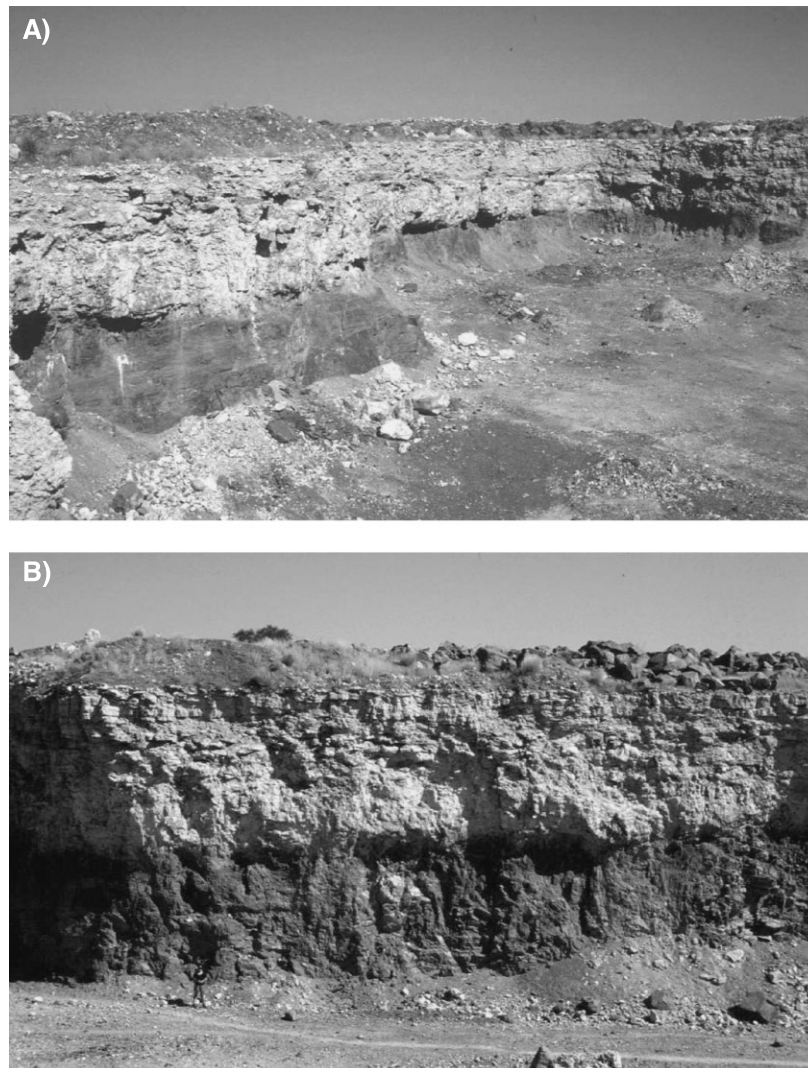


Figure 3. Views of Tswaane Quarry: (A) the east wall of the quarry including sample profile BOT 98/25; (B) the south of the quarry including profile BOT 98/26

silica, chalcedony, microquartz, micrite and microspar/sparite carbonate cements as well as late-stage silica and carbonate void-fills of various types. Counts for porosity only include an assessment of secondary porosity as no primary porosity appeared to be present. Descriptions of any variations in the fabric of samples were noted separately. The results of point-count analyses for Kang Pan are shown in Table I and for Tswaane in Tables II and III.

The bulk density of the remaining half of each sample from Tswaane Quarry was determined using Archimede's principle, calculated by dividing the mass of each air-dried sample by the volume of liquid instantaneously displaced when lowered into water. Geochemical analyses of samples from Kang Pan and Tswaane Quarry were undertaken by X-ray fluorescence spectrometry (XRFS) at the Analytical Geochemistry Laboratories of the British Geological Survey, Keyworth, UK. XRFS analyses were carried out on fused glass beads for major and minor elements and pressed powder pellets for trace elements. Samples were jaw-crushed, riffle-split, milled in an agate mill, agate-ball-milled and dried overnight at 105 °C prior to the generation of fused discs and powder pellets. Loss on ignition was determined after one hour at 1050 °C. The lower limit of detection for trace elements is approximately 5 ppm. Results of geochemical analyses are shown in Tables IV and V for Kang Pan

and Tables VI and VII for Tswaane Quarry. The median values of selected major and minor elements for grouped calcrete, silcrete, cal-silcrete and bedrock samples are shown in Table VIII.

In order to calculate the changes in element concentration associated with calcrete and silcrete formation, the isocon method (Gresens, 1967; Grant, 1986) was used. This is described in detail by Webb and Golding (1998) and is, therefore, only outlined here. Under this method, concentrations of major and trace elements within one material are plotted against those in another. Typically, an altered material like a duricrust is compared with the parent lithology, but the technique can be used to compare any two related lithologies, e.g. calcrete and silcrete in the present study. A straight line (the isocon) is plotted onto this graph from the origin, passing through all elements that are considered to have been immobile. Elements which plot above or below the isocon have been either respectively enriched or depleted in the material plotted on the vertical axis. The gradient of the isocon can be used to identify whether any mass change has occurred during alteration from one material to another, with a slope value close to 1 suggesting isovolumetric replacement (providing the densities of the two materials are approximately the same). To apply this method to the development of the Kalahari calcrete, silcrete and intergrade duricrusts, an immobile element that is relatively evenly distributed throughout these materials must be chosen to act as a reference. Under hydrothermal alteration, Al, Ti and Zr are usually immobile. However, there is strong evidence to suggest that loss of Al and redistribution or gain of Ti may occur during silcrete formation (e.g. Hutton *et al.*, 1978; Webb and Golding, 1998). In comparison, Zr is relatively immobile (Summerfield, 1984), apart from under extremely high or low pH conditions (Thornber, 1992). Some studies of Australian silcretes (e.g. Butt, 1985) have identified slight etching of zircon grains, but any chemical transport of Zr has been very limited. As such, Zr has been selected as a reference element for the purposes of this study. Furthermore, inspection of thin-sections suggests that zircon grains are widely distributed throughout the duricrusts present at the study site, and display no evidence of etching.

MACRO- AND MICROMORPHOLOGICAL RESULTS: KANG PAN

General characteristics

The quarry at Kang Pan (Figure 2A) exposes a 5.5 m sequence of highly indurated, crystalline calcrete, cal-silcrete and sil-calcrete duricrusts, all of which developed within Kalahari Group quartz sand host sediments. The profile is well-jointed, with a more massive blocky appearance near the base and thinner layers towards the surface. The exposure is dominated by silica-rich duricrusts in lower sections which grade upwards into materials with more calcareous cements towards the top of the profile. However, this gradation is not progressive. Silicification occurs in distinct zones in lower sections of the profile, both at the edges and towards the centres of inter-joint blocks. This gives lower parts of the exposure a mottled dark grey to black to pink appearance, in comparison with the otherwise white to pale grey upper calcrete units (Figure 2B). Zones of silicification commonly have sharp boundaries with adjacent carbonate-cemented materials, suggesting that the extent of silicification is determined by the penetration of a wetting front into the profile. In many cases, areas of silica-dominated cement are rimmed by a thin (<10 mm) zone of powdery calcite (Figure 2B), which appears to have been mobilized during silicification and subsequently precipitated marginal to the silicified zone. Additional late-stage silicification also appears to have been focused along cracks and fractures, mainly within upper parts of the profile, leading to the development of pale green silica-carbonate precipitates within and adjacent to some joints. One sample of silicified material from within a joint at a height of approximately 3 m has been analysed in thin-section (BOT 98/29/12; Table I).

Micromorphology

The exposure at Kang Pan contains a complex combination of silica- and carbonate-cemented duricrusts. The sequence essentially consists of a microsparite- to sparite-dominated alpha-fabric calcrete developed within quartz sand host sediments (Figure 4A), which has been partially to extensively silicified (as summarized in the point-count data in Table I). Lower parts of the profile contain more sparry calcite crystals with a higher percentage of microspar and micrite present towards the top. The original carbonate fabric (prior to silicification) appears to have been relatively simple throughout the profile, with a complete absence of pedogenic and other

Table I. Point-count data for silcrete–calcrete intergrade duricrusts from Kang Pan

Sample	Lithology	Height (m)	Quartz grains	Secondary porespace	Cryptocrystalline silica cement	Chalcedonic silica cement	Microquartz cement	Grain- coating silica	Late stage void-filling silica	Total silica cement	Micrite cement	Microspar/ sparite cement	Grain- coating calcite	Late-stage void-filling calcite	Total carbonate
BOT 98/29/11	Cal-silcrete	5.0	24.0	0	1.0	25.7	0	1.0	10.7	38.4	5.3	28.0	2.0	2.3	37.6
BOT 98/29/10	Calcrete	4.5	9.0	2.3	0	0	0	0	0	0	44.7	42.3	1.7	0	88.7
BOT 98/29/9	Calcrete	4.0	17.3	1.0	1.0	13.3	0	1.3	1.0	16.6	12.7	51.0	0.7	0.7	64.4
BOT 98/29/8	Calcrete	3.5	17.3	0	0	5.7	0	0	0	5.7	1.3	74.3	1.4	0	77.0
BOT 98/29/7	Calcrete	3.0	24.6	0.7	1.7	8.3	2.3	1.4	0	13.7	25.7	32.3	3.0	0	61.0
BOT 98/29/6	Calcrete	2.5	16.0	0.7	0	0	0	0	0	0	3.0	79.3	1.0	0	83.3
BOT 98/29/5	Cal-silcrete	2.0	31.0	1.0	2.0	34.6	0	2.0	0	38.6	3.0	25.3	1.1	0	29.4
BOT 98/29/4	Cal-silcrete	1.5	26.3	0.3	0.3	20.0	0	1.0	1.0	22.3	1.7	49.0	0	0.4	51.1
BOT 98/29/3	Cal-silcrete	1.0	38.3	0	2.0	12.3	0	1.7	0	16.0	25.0	20.7	0	0	45.7
BOT 98/29/2	Cal-silcrete	0.5	56.3	0	2.3	33.0	0.3	1.7	1.7	39.0	0	3.0	1.7	0	4.7
BOT 98/29/1	Cal-silcrete	0	44.3	0	7.7	32.7	0	2.0	5.3	47.7	1.3	5.6	0	1.1	8.0
BOT 98/29/12	Sil-calcrete	3.0	20.7	0.7	1.0	24.0	0	2.3	1.3	28.6	5.0	43.0	1.7	0.3	50.0

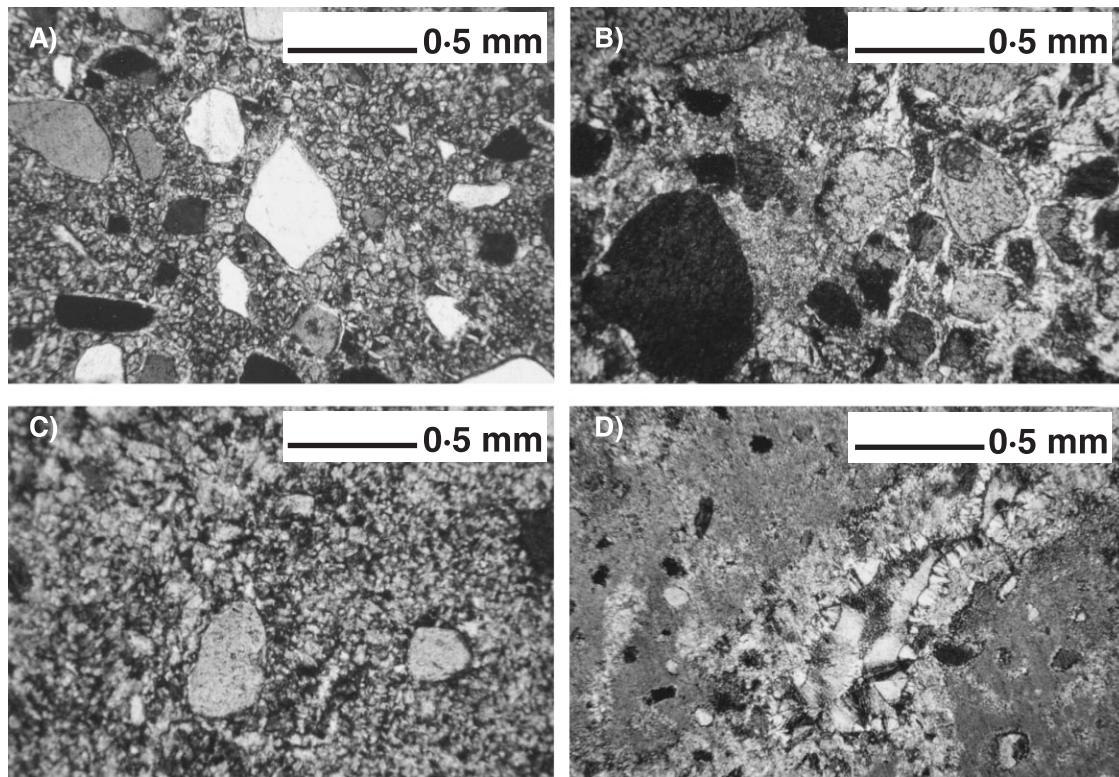


Figure 4. Thin-section photomicrographs of samples from Kang Pan: (A) unaltered alpha-fabric calcrite (BOT 98/29/1); (B) patchy replacement of carbonate cement (left of view) by chalcidonic and cryptocrystalline silica (right of view) with sharp boundary between silica and carbonate cements (BOT 98/29/3); (C) diffuse replacement of carbonate cement by chalcedony (BOT 98/29/5); (D) alpha-fabric calcrite with void containing layered opaline and chalcedonic silica overlain by sparry calcite and infilled with length-slow fibrous chalcedony (BOT 98/29/9)

organic structures. A number of trends can be identified throughout the section (Table I). Firstly, the profile is relatively well-indurated, with the total secondary porespace rarely exceeding 1 per cent. Secondly, the percentage of host quartz grains declines from a peak value of around 50 per cent of the duricrust volume at the base of the quarry to under 10 per cent in upper sections. Thirdly, silica cements dominate lower sections of the exposure but decline in abundance upwards, with the exception of relatively high values at 2 and 5 m from the base. This is in almost inverse relationship to the percentage of carbonate cement present, which increases up-profile.

These general trends mask considerable complexity, both within the types of cements present and the cementation sequence. The lowermost sections of the profile are dominated by cal-silcrete, which appears to have formed as a result of extensive replacement of calcite crystals by chalcedony and minor amounts of cryptocrystalline silica, as well as by the precipitation of chalcedony and opaline silica within void spaces. Middle and upper sections of the profile mainly consist of duricrusts with calcareous cements and evidence of only localized silica replacement, whilst the uppermost sample is extensively silicified, with silica occurring both as a replacive cement and within complex late-stage void-fills. Silicification is also dominant within the sample of silica-carbonate material precipitated along a joint (BOT 98/29/12); this contains chalcedonic silica cements in proportions comparable with materials from the lower part of the profile.

Silica replacement occurs throughout the exposure and takes two main forms. Firstly, patches of chalcedony and, occasionally, cryptocrystalline silica or microquartz cement, often with very sharp cement boundaries, are found within the precursor sparite matrix (Figure 4B). In places these siliceous patches dominate the intergrade duricrust matrix and are the main form of silicification visible in hand specimen and at the profile scale (Figure 2A,B). These patches would appear to represent the wholesale replacement of pre-existing calcite cements by silica. This form of replacement is also dominant in the late-stage siliceous material sampled from within a joint. Evidence at the

profile scale suggests that some of the carbonate mobilized during the silicification process is precipitated outside the zone of silica-rich cement, but there is little clear evidence for this in thin-section. The second form of replacement is where more diffuse silicification of the existing calcrete appears to have occurred, with chalcedony and cryptocrystalline silica either completely or partly replacing individual sparite crystals, or even coating crystals, to produce a matrix with fretted calcite rhombs 'floating' in a silica cement (Figure 4C). This may be a stage on the route to the complete replacement of a calcite-dominated matrix by larger silica patches. Both forms of replacement, do, however, occur within individual samples, suggesting that they may be discrete modes.

Late-stage void-filling cements vary in composition throughout the profile, with the greatest complexity occurring in samples from lower sections. Void-fills occur in both cracks and pores and commonly consist of alternating layers of silica and carbonate, reflecting complex changes in porewater chemistry and pH during the latter stages of cementation of the profile. Voids within BOT 98/29/1, for example, are lined by chalcedonic silica, partially infilled by crystalline calcite and have acicular quartz crystals growing within their centre, whilst the late-stage silicified sample from within a joint (BOT 98/29/12) contains layered calcite–chalcedony–calcite fills. In contrast, void-fills towards the top of the profile (BOT 98/29/9; Figure 4D) are lined by opaline and chalcedonic silica which is overlain by sparry calcite, with the void filled by optically length-slow fibrous chalcedony, suggesting formation in an alkaline setting (Folk and Pittman, 1971).

Profile development

The simple calcrete fabric, dense cementation and relatively coarse calcite crystal size present in lower parts of the profile, suggest that the duricrust sequence at Kang Pan was initially generated as a non-pedogenic groundwater calcrete in a pan-marginal or pan-floor setting. If crystal size is taken as a broad proxy for the duration of wetting (Wright and Tucker, 1991), calcite precipitation would appear to have taken place mainly at or below the water table. The micritic cements in the upper parts of the profile suggest a near-surface setting, with carbonate precipitation driven by evaporation. The up-profile decrease in the percentage of host sediments would appear to reflect displacement of clasts during the development of the original carbonate cement. This precursor calcrete was substantially silicified in its lower- and uppermost sections and subsequently experienced further localized alteration. Diagenetic alteration occurred through the partial replacement of calcite crystals by various silica polymorphs, mainly below the water table, allowing the total replacement of large patches of carbonate cement. Replacement may have been influenced by the location of joints and fractures within the calcrete, although more diffuse replacement away from fractures suggests that silicification may also have occurred within saturated calcrete masses. The presence of complex alternating silica and calcite late-stage void-linings and void-fills is indicative of the circulation of silica- and carbonate-rich solutions throughout the intergrade duricrust profile, suggesting fluctuations in porewater pH. The lack of any consistent sequence of void-linings may indicate the partial or complete cementation of some fractures during diagenesis, preventing the passage of solutions through the profile.

The distribution of secondary silica features throughout the profile provides an indication of the role of temporal variations in water table height during the cement development. Replacement near the base of the profile was most likely associated with periods when the water table was elevated relative to its present position. Furthermore, the extent of silicification is suggestive of a, possibly lengthy, period of water table stability. In contrast, near-surface silicification was most probably associated with occasional inundation of the pan surface by silica-rich solutions, which both saturated upper sections of the calcrete and permeated into the underlying substrate. The presence of length-slow chalcedony within some void spaces may indicate that these solutions were of relatively high pH. Thus, silicification appears to have occurred at two levels, controlled by periodic inundation and fluctuations in positions of the water table.

MACRO- AND MICROMORPHOLOGICAL RESULTS: TSWAANE QUARRY

General characteristics

The aggregate quarry at Tswaane exposes a 3.5 to 4 m thick complex sequence of calcrete, silcrete and silcrete–calcrete intergrade duricrusts overlying up to 8 m of bedrock (Figure 3A,B). Three broad zones of

material can be distinguished at the profile scale. Basal sections of the exposure consist of purple to red Precambrian granitoid-gneiss, which grades upwards from unweathered bedrock into a superficially altered zone comprising slightly more friable bedrock. This is overlain by 3 to 3.5 m of pale green, variably indurated silcrete and cal-silcrete, which appears to have developed through the cementation and/or replacement of granitoid-gneiss and Kalahari Group sediments, as indicated by the occurrence of quartz sand grains and occasional bedrock fragments within the silcrete matrix. The proportion of bedrock fragments within this zone appears to decline upwards, with increasing dominance of Kalahari Group quartz sand within the middle to upper sections of the silcrete and overlying calcrete. The bedrock and siliceous duricrusts are capped by 0.5 to 1 m of creamy-white, relatively crumbly and friable calcrete. The three-dimensional relationship between the various components of the duricrust sequence and underlying bedrock has been observed through inspection of exposures in the quarry sides. The transition between bedrock and silcrete undulates over a vertical range of 1 to 2 m, and may reflect original topographic undulation of the gneiss surface. The progression from silcrete to calcrete is also spatially variable. Observation of the east side of the quarry, perpendicular to the Okwa Valley, reveals that the intersection between the green silcrete-dominated duricrust and white calcrete slopes at an angle of approximately 2° towards the valley axis. Carbonate penetration is also more extensive within some sections of the exposure, particularly on the north side of the quarry closest to the Okwa Valley.

Micromorphology

Point-count data and qualitative analyses of thin-sections for profiles BOT 98/25 (Table II) and BOT 98/26 (Table III) show a broadly consistent picture of silica and carbonate cement development, suggesting that similar processes have occurred throughout Tswaane Quarry to create the contemporary duricrust sequence. Thin-sections (Figure 5) from both profiles indicate that the Precambrian bedrock in the base of the pit is mostly unaltered, although opaque iron-oxide-rich minerals line cracks and voids in all samples. The proportion of opaque minerals within the bedrock remains relatively consistent in BOT 98/25 but increases upwards in profile BOT 98/26. Sample BOT 98/26/7, for example, immediately below the bedrock–silcrete interface, contains 28 per cent opaque minerals, which are most abundant at the intersections of fractures within the bedrock. Significantly, virtually no opaque minerals are present above the bedrock–silcrete interface in either profile. The only other evidence of bedrock alteration occurs at 4.5 and 5 m from the base of profile BOT 98/25 (sample BOT 98/25/6). The matrix here is dominated by displacive sparry calcite, which accounts for 67 per cent of the sample and locally brecciates the bedrock fabric (Figure 5A). Minor traces of chalcedony and opaque minerals are also present in some cracks and voids. The altered bedrock is pale green in colour, similar to the overlying silcrete and to the samples described above from Kang Pan. This is probably only a localized occurrence, because calcite is not present within the bedrock in profile BOT 98/26. Sample BOT 98/25/5 also contains small quantities of calcite within void spaces, not noted during point-counting; this is presumably a late-stage diagenetic feature.

The pale green siliceous duricrusts above the transition zone (samples BOT 98/25/8–13 and BOT 98/26/8–16) exhibit a complex history of development. Samples from both profiles contain variable (but always low) quantities of granitoid-gneiss fragments and sub- to well-rounded medium-grained quartz clasts. These are cemented by poorly ordered silica polymorphs such as cryptocrystalline silica, which constitute over 60 per cent of most thin-sections (Figure 5B). Minor quantities of microquartz are present in sample BOT 98/25/9 but chalcedony is almost entirely absent except in some void-fills. Two main silcrete fabrics are present, either separately or in combination, throughout the profile. The first is a smooth, sometimes banded, low-porosity, matrix-dominated, cryptocrystalline silica-cemented silcrete which is strongly suggestive of the direct replacement of a micritic alpha-fabric calcrete. The second fabric type consists of cryptocrystalline silica with a cracked and brecciated appearance cementing quartz grains and bedrock fragments. Areas of the silcrete exhibiting the latter fabric type are typically more porous and contain circular to elongate voids. Some parts also retain textures inherited by replacement of granitoid-gneiss and calcrete, including ‘ghosts’ of crystal outlines from metamorphic host materials and possible calcrete glaebular structures. Within both silcrete fabric types, the pale green coloration is distributed evenly throughout the sample, as opposed to being present in discrete areas of the sample or in association with specific mineral grains.

In addition to host materials and cryptocrystalline silica cement, almost all silcrete samples contain a proportion of carbonate cement. Calcite appears to have been mostly precipitated after the main phase of silcrete

Table II. Point-count data for calcrete, silcrete and granitoid-gneiss from Tswaane Quarry sample profile BOT 98/25

Sample	Lithology	Height (m)	Bedrock/lithic fragments	Quartz grains	Secondary porespace	Cryptocrystalline silica cement	Chalcedonic silica cement	Microquartz cement	Late-stage void-filling silica	Total silica cement	Micrite cement	Microspar/sparite cement	Late-stage void-filling calcite	Total carbonate	Late-stage iron oxide in voids
BOT 98/25/14	Calcrete	9.0	0	4.0	0.6	0	0	0	0	0	95.4	0	0	95.4	0
BOT 98/25/13	Silcrete	8.5	3.0	3.5	4.0	82.5	0	0	1.5	84.0	0	0	5.5	5.5	0
BOT 98/25/12	Cal-silcrete	8.0	2.0	5.9	1.0	80.1	0	0	0	80.1	0	3.5	7.5	11.0	0
BOT 98/25/11	Silcrete	7.5	0	3.5	1.0	80.0	0	0	0	80.0	0	10.5	5.0	15.5	0
BOT 98/25/10	Silcrete	7.0	1.0	5.5	2.0	83.0	0	0	0	83.0	0	6.0	2.5	8.5	0
BOT 98/25/9	Silcrete	6.5	0	7.5	6.0	82.0	0	1.0	2.0	85.0	0	0	1.5	1.5	0
BOT 98/25/8	Silcrete	6.0	5.5	5.5	5.0	83.0	0	0	0	83.0	0	0	0	0	1.0
BOT 98/25/7	Bedrock	5.5	90.0	0	2.0	0	0	0	0	0	0	0	0	0	8.0
BOT 98/25/6	Calcified bedrock	5.0	26.5	2.5	2.0	0	0	0	0	0	0	67.0	0	67.0	2.0
BOT 98/25/5	Bedrock	4.5	93.0	0	0	0	0	0	0	0	0	0	0	0	7.0
BOT 98/25/4	Bedrock	4.0	92.0	0	0	0	0	0	0	0	0	0	0	0	8.0
BOT 98/25/3	Bedrock	3.5	92.5	0	0	0	0	0	0	0	0	0	0	0	7.5
BOT 98/25/2	Bedrock	3.0	90.5	0	0	0	0	0	0	0	0	0	0	0	9.5
BOT 98/25/1	Bedrock	2.5	88.5	0	0	0	0	0	0	0	0	0	0	0	11.5

Table III. Point-count data for calcrete, silcrete and granitoid-gneiss from Tswaane Quarry sample profile BOT 98/26

Sample	Lithology	Height (m)	Bedrock/lithic fragments	Quartz grains	Secondary porespace	Cryptocrystalline silica cement	Chalcedonic silica cement	Microquartz cement	Late-stage void-filling silica	Total silica cement	Micrite cement	Microspar/sparite cement	Late-stage void-filling calcite	Total carbonate	Late-stage iron oxide in voids
BOT 98/26/16	Cal-silcrete	9.0	0	6.5	2.5	74.5	0	0	4.5	79.0	0	5.0	7.0	12.0	0
BOT 98/26/15	Silcrete	8.5	0	4.0	2.0	87.5	0	0	0	87.5	0	5.0	1.5	6.5	0
BOT 98/26/14	Cal-silcrete	8.0	1.5	2.0	2.5	78.0	0	0	1.0	79.0	0	3.0	12.0	15.0	0
BOT 98/26/13	Silcrete	7.5	0	10.0	4.0	74.0	0	0	2.0	76.0	0	3.5	6.5	10.0	0
BOT 98/26/12	Cal-silcrete	7.0	2.5	8.0	3.0	51.0	0	0	0	51.0	0	35.5	0	35.5	0
BOT 98/26/11	Silcrete	6.5	0	5.5	1.5	90.0	0	0	2.0	92.0	0	0	1.0	1.0	0
BOT 98/26/10	Cal-silcrete	6.0	0	6.0	2.0	79.0	0	0	0	79.0	0	10.0	3.0	13.0	0
BOT 98/26/9	Cal-silcrete	5.5	25.5	6.0	3.0	60.5	0	0	0	60.5	0	5.0	0	5.0	0
BOT 98/26/8	Silcrete	5.0	1.5	4.5	3.0	90.0	0	0	0	90.0	0	1.0	0	1.0	0
BOT 98/26/7	Altered bedrock	4.5	72.0	0	0	0	0	0	0	0	0	0	0	0	28.0
BOT 98/26/6	Altered bedrock	4.0	86.5	0	0	0	0	0	0	0	0	0	0	0	13.5
BOT 98/26/5	Altered bedrock	3.5	85.0	0	0	0	0	0	0	0	0	0	0	0	15.0
BOT 98/26/4	Bedrock	3.0	94.0	0	0	0	0	0	0	0	0	0	0	0	6.0
BOT 98/26/3	Bedrock	2.5	93.0	0	0	0	0	0	0	0	0	0	0	0	7.0
BOT 98/26/2	Bedrock	2.0	92.0	0	0	0	0	0	0	0	0	0	0	0	8.0
BOT 98/26/1	Bedrock	1.5	89.5	0	0	0	0	0	0	0	0	0	0	0	10.5

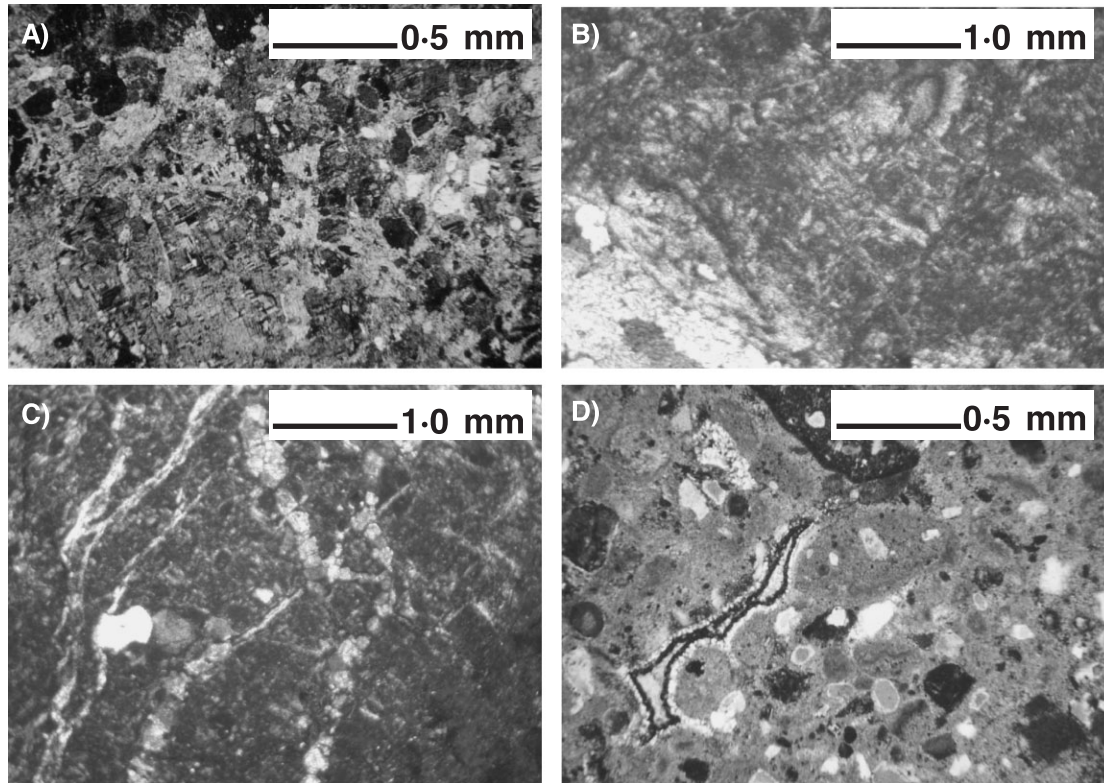


Figure 5. Thin-section photomicrographs of samples from Tswaane Quarry: (A) granitoid-gneiss bedrock brecciated by sparry calcite (BOT 98/25/6); (B) silcrete with cryptocrystalline and chalcedonic silica cement plus a fragment of unaltered bedrock (BOT 98/25/8); (C) silcrete with gravitational stringers of sparite precipitated within voids (BOT 98/25/11); (D) alpha-fabric calcrete with void filled with layered opaline silica and sparite (BOT 98/26/16)

replacement; it is, however, possible that components of the carbonate-cemented horizons immediately above the green siliceous duricrusts predate the phase of silicification. Calcite content is commonly in the range of 5 to 15 per cent, although one sample (BOT 98/25/12) contains up to 35 per cent microsparite and sparite. Calcite cements are present in three forms. Firstly, many silcreted horizons are brecciated by microsparite or sparite, particularly those in the uppermost parts of the silcrete mass. These carbonate cements often appear laminated and have developed incrementally. Many samples contain evidence of fretting of the margins of brecciated silcrete fragments, suggesting partial replacement during cementation. This produces, in places, a complex fabric in which fretted silcrete fragments, themselves containing evidence of replaced calcrete structures, are cemented by various forms of calcite. Secondly, calcite occurs as vertically oriented strings of sparite crystals along cracks (e.g. BOT 98/25/11; Figure 5C) and as diffuse individual calcite rhombs within the cryptocrystalline silica matrix (e.g. samples BOT 98/26/12 and 15). The latter of these calcite textures is similar in appearance to some of the diffuse replacement features described from Kang Pan. Thirdly, calcite also occurs as late-stage void-fills, often in conjunction with silica precipitation. Void-fills are present throughout both profiles but appear to increase in middle to upper sections of the green silcrete mass. The most common form is a micritic calcite void-lining overlain by sparite which may completely fill the remaining porespace.

The top of profile BOT 98/25 comprises a micrite-dominated alpha-fabric calcrete with a relatively simple microcrystalline structure. The calcrete has developed within Kalahari Group quartz sand host sediments, with no bedrock fragments present. In contrast, the uppermost sample from profile BOT 98/26 is less well calcified. This duricrust is technically a cal-silcrete and is cemented by cryptocrystalline silica and microsparite. Complex layered quartz and sparite void fills (Figure 5D) are present, indicating the late-stage circulation of silica- and

carbonate-rich porewaters. Secondary porosity is relatively low at the top of both profiles and, in common with the underlying silcrete, neither sample appears to contain pedogenic structures.

Profile development

On the basis of the preceding micromorphological evidence, the duricrust suite exposed at Tswaane Quarry initially developed through the calcium carbonate cementation in a non-pedogenic setting of a sequence of Kalahari Group sediments mixed with minor quantities of Precambrian granitoid-gneiss. As at Kang Pan, parts of this calcrete were then completely or partially replaced by silcrete to produce a complex composite profile. The preservation of inherited bedrock and calcrete structures within the silcrete fabric suggests that development progressed by non-pedogenic groundwater silicification mechanisms. The inheritance of bedrock textures within the silcrete is particularly significant as this has not been identified in the Kalahari despite being documented in Australia (Watts, 1978) and along the Cape coast in South Africa (Summerfield, 1984). However, it should be noted that the main bulk of the bedrock has not been silicified, only the immediately overlying sediment which consists of a mixture of bedrock fragments and Kalahari Group quartz grains. The period of silcrete formation was followed by a further phase(s) of non-pedogenic calcrete development, which was accompanied by the gravitational precipitation of macrocrystalline calcite within cracks and voids and as diffuse crystals in the immediately underlying silcrete and localized areas of the bedrock. The general thickening of this calcrete towards the Okwa Valley suggests that calcretization occurred in association with lateral and/or vertical movement of solutions from the valley. Silica- and carbonate-rich porewaters appear to have remained in circulation subsequently, leading to the precipitation of complex sparitic and chalcedonic void-fills within calcrete void spaces.

This broad diagenetic sequence is also supported by macromorphological evidence. The approximately horizontal lower and gently sloping upper boundaries of the silcrete are strongly suggestive of a water table influence upon silicification, with silcrete development occurring at depth beneath a former valley floor prior to major incision of the Okwa. Previous investigations along the Okwa (e.g. Nash *et al.*, 1994b) have identified that silcrete outcrops are almost entirely restricted to the area around the Precambrian inlier at Tswaane. At this location, bedrock crops out at the surface in a region otherwise dominated by Kalahari Group sediments (Aldiss and Carney, 1992). It is possible therefore that, as in other Kalahari dry valleys (Shaw and de Vries, 1988; Nash *et al.*, 1994a), silcrete development was restricted to a zone where groundwater moving laterally beneath the valley floor was forced upwards. The precise mechanisms triggering silica precipitation at such sites are unclear, but may involve evaporation and near-surface pH changes, as in pan-type settings. The downslope thickening of the non-pedogenic calcrete present at the top of the quarry indicates that later calcrete development was also directly influenced by the presence of a drainage-line, in this case probably after a phase of incision. Such thickening of calcretes in close proximity to valleys is common in the Kalahari and has been recognized in other dry valley systems such as the Rooibrak and Mmone-Quoxo (Mallick *et al.*, 1981; Nash *et al.*, 1994a). Calcite precipitation must have occurred both near to and below the water table, to produce the micrite-dominated surface calcretes as well as more crystalline sparite cements at depth within the underlying silcrete.

GEOCHEMISTRY: KANG PAN AND TSWAANE QUARRY

Despite the differences in macro- and micromorphology noted above, the three duricrust profiles from Kang Pan and Tswaane Quarry have very similar chemical compositions, and, as such, are considered together. Analyses of the geochemical data shown in Tables IV–VIII can be used to (a) ascertain the likely contribution of bedrock (both as a host material and source of cementing solutions) to the development of the duricrust profiles; (b) distinguish differences between various duricrust types; and (c) further supplement micromorphological evidence concerning the broad environment of formation of duricrusts from the two study locations.

Comparisons of the major and minor element analyses of duricrusts from both sites with those from the granitoid-gneiss at Tswaane Quarry suggest that bedrock made little contribution to the development of duricrusts at Tswaane, either in solid form or through the supply of weathered solutes. This proposition is made on the basis of two lines of evidence. Firstly, analyses of samples from the basal sections of the two profiles at Tswaane (Tables VI and VII) indicate that the bedrock is geochemically uniform (Figure 6), suggesting a lack of chemical weathering profile development. This is further supported by the relatively low loss-on-ignition (LOI) values for

Table IV. Major element analyses for silcrete–calcrete intergrade duricrusts from Kang Pan (profile BOT 98/29)

Sample	Lithology	Height (m)	Major elements (%)												
			SiO ₂	TiO ₂	Al ₂ O ₃	Fe ₂ O ₃ t	Mn ₃ O ₄	MgO	CaO	Na ₂ O	K ₂ O	P ₂ O ₅	SO ₃	BaO	LOI
BOT 98/29/11	Cal-silcrete	5.0	50.62	0.08	0.93	0.43	<0.01	1.77	24.35	<0.05	0.35	0.01	<0.1	0.04	21.22
BOT 98/29/10	Calcrete	4.5	29.98	0.06	0.76	0.37	0.02	1.60	36.14	<0.05	0.30	0.03	<0.1	0.03	30.31
BOT 98/29/9	Calcrete	4.0	46.55	0.09	1.01	0.66	0.06	1.77	26.17	<0.05	0.50	0.01	<0.1	0.31	22.24
BOT 98/29/8	Calcrete	3.5	33.29	0.06	0.67	0.39	0.02	1.27	34.80	<0.05	0.25	<0.01	<0.1	0.04	28.67
BOT 98/29/7	Calcrete	3.0	30.04	0.07	0.87	0.48	0.02	1.56	35.98	<0.05	0.35	0.01	<0.1	0.04	30.10
BOT 98/29/6	Calcrete	2.5	35.87	0.06	0.70	0.37	0.01	1.26	33.45	<0.05	0.27	<0.01	<0.1	0.03	27.58
BOT 98/29/5	Cal-silcrete	2.0	74.56	0.07	0.91	0.47	0.02	1.55	10.86	<0.05	0.35	<0.01	<0.1	0.04	10.23
BOT 98/29/4	Cal-silcrete	1.5	50.95	0.09	1.47	0.52	0.02	2.73	22.83	0.06	0.47	<0.01	<0.1	>0.02	20.36
BOT 98/29/3	Cal-silcrete	1.0	65.57	0.09	1.33	0.49	0.01	1.82	15.42	0.06	0.50	<0.01	<0.1	0.03	14.03
BOT 98/29/2	Cal-silcrete	0.5	78.04	0.09	1.35	0.47	0.01	2.78	7.09	0.08	0.54	<0.01	<0.1	0.04	8.74
BOT 98/29/1	Cal-silcrete	0	80.95	0.09	1.73	0.50	0.01	2.48	5.54	0.11	0.58	<0.01	<0.1	0.03	7.07

LOI, loss on ignition

Table V. Minor element analyses for silcrete–calcrete intergrade duricrusts from Kang Pan (profile BOT 98/29)

Sample	Height (m)	Minor elements (ppm)													
		Ni	Cu	Zn	Ga	As	Rb	Sr	Y	Zr	Nb	Hf	Pb	Th	U
BOT 98/29/11	5.0	5	8	48	<1	<1	10	249	6	56	2	1	3	<1	2
BOT 98/29/10	4.5	7	7	10	<1	<1	9	434	6	48	1	<1	2	<1	6
BOT 98/29/9	4.0	9	10	30	<1	<1	12	299	13	76	2	2	4	<1	3
BOT 98/29/8	3.5	5	12	146	<1	<1	6	299	9	45	1	1	4	<1	<1
BOT 98/29/7	3.0	6	13	109	<1	<1	9	312	16	51	<1	1	4	<1	<1
BOT 98/29/6	2.5	4	11	100	<1	<1	8	206	5	39	1	<1	<1	<1	1
BOT 98/29/5	2.0	5	10	111	1	<1	10	100	5	55	<1	2	2	<1	5
BOT 98/29/4	1.5	10	12	45	2	1	13	217	10	66	1	2	5	<1	<1
BOT 98/29/3	1.0	7	8	18	2	<1	14	92	12	80	2	1	4	1	<1
BOT 98/29/2	0.5	8	8	16	<1	1	14	142	5	75	2	1	3	<1	<1
BOT 98/29/1	0	12	9	21	3	2	15	54	5	79	2	2	3	1	2

the bedrock (<0.75 per cent) which indicate a low hydrous and carbonate mineral content and, therefore, little alteration of feldspars and micas to clays and carbonates. Even the superficially altered, more friable bedrock samples show almost no conclusive evidence for chemical weathering, as their median composition is almost identical to that of fresh granitoid-gneiss (Table VIII). As such, the granitoid-gneiss is unlikely to have been a major source of species for the silicification and calcification of the overlying sand-rich sediments. It is possible that a weathering profile may have existed prior to the deposition of the Kalahari Group sediments and that this weathered profile was subsequently stripped. This is, however, unlikely given the lack of evidence of large-scale incision into pre-Kalahari Group formations in this region. The limited extent of weathering is most probably, therefore, a product of the long-term arid to semi-arid climate experienced within the Kalahari throughout much of the Quaternary and Late Tertiary (Thomas and Shaw, 1991).

The second indication that the granitoid-gneiss made little contribution to the development of duricrusts at Tswaane is the distinct difference in chemical signature of the two sets of materials. The bedrock is geochemically very different from the calcrete, silcrete and intergrade duricrusts at both Tswaane and Kang Pan (Tables V–VIII; Figure 6), as it contains substantially higher levels of Al, Ti, Fe, Na, K, Rb, Zr, Y, Nb and Pb, but lower Mg, Ca, LOI, Sr (particularly in comparison to the calcretes), Ni and Cu. The lack of Ca in the granitoid-gneiss and the lack of depletion of Si, in particular, suggest that these elements were, for the most part, supplied to the overlying duricrusts from external sources. However, the lowermost silcrete samples from both profiles at Tswaane Quarry show some geochemical features intermediate between the granitoid-gneiss and the other duricrusts (Table VIII), and contain both quartz sand grains and bedrock fragments within the silcrete matrix. These silcretes have higher levels of Zr (Figure 7A), Al, K, Na, Rb, Pb, Nb and Y than are typical of the other duricrust samples, probably due to incorporation of zircon and feldspar (and/or weathered clay derived from the feldspar) from the underlying granitoid-gneiss. The ratio of the physical contributions of the granitoid-gneiss and Kalahari Group sands to the lower silcrete is approximately 1:3, calculated from the median Zr concentrations of the bedrock (384 ppm), lower silcrete (144 ppm) and remaining duricrusts (41 ppm, representative of the Kalahari Group sands), assuming that Zr is chemically immobile (Webb and Golding, 1998; Balan, *et al.*, 2001).

Overall, it would appear that the duricrusts at Tswaane Quarry (apart from the basal silcretes) were developed within precursor Kalahari Group sediments, with cementing agents supplied laterally as opposed to vertically from underlying bedrock. The same conclusion applies to the duricrusts at Kang Pan, which have a very similar geochemistry to those at Tswaane. The majority of calcrete, silcrete and intergrade duricrust samples from both sites contain comparable levels of some elements, particularly Zr (Table VIII, Figure 7A) as well as other trace elements (Pb, Nb, Ni, Cu). The duricrusts are also all distinguished by very low concentrations of Na (Table VIII). The precise source of cementing agents at each site is unclear. The Okwa Valley rises in an area of Precambrian silicate-rich bedrock in eastern Namibia before cutting through the Kalahari Group sediments in Botswana. As such, it is possible that silica was supplied from distant weathered sources. This is unlikely to be

Table VI. Major element analyses for calcrete, silcrete and granitoid-gneiss from Tswaane Quarry

Sample	Lithology	Height (m)	Density (g cm ⁻³)	Major elements (%)												
				SiO ₂	TiO ₂	Al ₂ O ₃	Fe ₂ O _{3t}	Mn ₃ O ₄	MgO	CaO	Na ₂ O	K ₂ O	P ₂ O ₅	SO ₃	BaO	LOI
<i>Profile BOT 98/25</i>																
BOT 98/25/14	Calcrete	9.0	2.368	9.42	0.05	0.51	0.28	0.03	0.86	48.37	<0.05	0.15	0.02	<0.1	0.03	39.81
BOT 98/25/13	Silcrete	8.5	1.896	84.62	0.18	3.90	2.01	0.02	1.88	0.61	0.08	2.79	<0.01	<0.1	0.05	3.01
BOT 98/25/12	Cal-silcrete	8.0	2.345	79.07	0.13	3.04	1.54	0.03	1.63	4.98	0.08	2.23	<0.01	<0.1	0.03	6.26
BOT 98/25/11	Silcrete	7.5	2.390	85.14	0.10	2.48	1.41	0.02	1.53	2.22	<0.05	1.91	<0.01	<0.1	0.13	4.05
BOT 98/25/10	Silcrete	7.0	2.288	82.70	0.15	3.34	2.60	0.05	1.56	1.67	0.08	2.91	<0.01	<0.1	0.06	4.10
BOT 98/25/9	Silcrete	6.5	2.096	84.70	0.12	2.87	1.90	0.04	1.25	2.06	0.10	2.38	<0.01	<0.1	0.06	3.72
BOT 98/25/8	Silcrete	6.0	1.885	84.46	0.15	5.15	1.87	0.06	0.87	0.50	0.83	3.42	<0.01	<0.1	0.09	1.82
BOT 98/25/7	Bedrock	5.5	2.625	74.04	0.24	11.80	3.22	0.02	0.18	0.19	3.14	5.49	<0.01	<0.1	0.18	0.64
BOT 98/25/6	Calcified bedrock	5.0	2.616	29.88	0.12	3.71	1.83	0.08	1.47	32.21	0.61	2.50	0.02	<0.1	0.05	27.02
BOT 98/25/5	Bedrock	4.5	2.500	73.64	0.24	11.84	3.12	0.03	0.20	0.28	3.16	5.60	<0.01	<0.1	0.19	0.65
BOT 98/25/4	Bedrock	4.0	2.620	74.79	0.22	11.39	3.10	0.02	0.16	0.29	3.09	5.27	<0.01	<0.1	0.20	0.59
BOT 98/25/3	Bedrock	3.5	2.631	71.52	0.18	13.21	3.43	0.04	0.12	0.17	3.73	5.80	<0.01	<0.1	0.25	0.62
BOT 98/25/2	Bedrock	3.0	2.628	75.53	0.21	11.17	2.84	0.04	0.12	0.40	3.24	4.77	0.01	<0.1	0.22	0.71
<i>Profile BOT 98/26</i>																
BOT 98/26/16	Cal-silcrete	9.0	2.481	79.10	0.04	0.94	0.49	0.01	1.51	7.95	<0.05	0.60	0.01	<0.1	0.19	8.22
BOT 98/26/15	Silcrete	8.5	2.423	88.92	0.09	1.79	0.87	<0.01	0.89	1.48	<0.05	1.24	<0.01	<0.1	0.20	3.31
BOT 98/26/14	Cal-silcrete	8.0	2.395	81.67	0.07	1.40	0.67	0.03	1.69	5.40	<0.05	0.98	<0.01	<0.1	0.32	6.85
BOT 98/26/13	Silcrete	7.5	2.386	85.76	0.09	1.94	0.90	0.02	1.16	3.34	0.05	1.36	<0.01	<0.1	0.20	4.63
BOT 98/26/12	Cal-silcrete	7.0	2.409	70.09	0.10	2.09	1.09	0.04	5.52	6.84	<0.05	1.46	<0.01	<0.1	0.05	11.70
BOT 98/26/11	Silcrete	6.5	2.293	87.96	0.11	2.51	1.44	0.02	1.73	0.45	0.07	1.77	<0.01	<0.1	0.09	2.91
BOT 98/26/10	Cal-silcrete	6.0	2.340	56.06	0.09	4.46	1.39	0.06	7.54	9.92	0.70	2.80	<0.01	<0.1	0.07	16.16
BOT 98/26/9	Cal-silcrete	5.5	2.036	74.54	0.11	3.24	1.78	0.06	4.12	4.10	0.32	2.40	<0.01	<0.1	0.06	8.25
BOT 98/26/8	Silcrete	5.0	2.097	85.33	0.15	3.69	2.21	0.07	1.24	0.55	0.43	2.89	<0.01	<0.1	0.07	2.46
BOT 98/26/7	Altered bedrock	4.5	2.643	72.90	0.22	11.78	4.26	0.02	0.13	0.12	3.21	5.46	<0.01	<0.1	0.37	0.45
BOT 98/26/6	Altered bedrock	4.0	2.640	74.60	0.22	11.12	3.55	0.02	0.11	0.10	2.40	6.07	<0.01	<0.1	0.32	0.47
BOT 98/26/5	Altered bedrock	3.5	2.635	73.54	0.26	11.55	4.52	0.03	0.15	0.11	3.23	5.20	<0.01	<0.1	0.26	0.41
BOT 98/26/4	Bedrock	3.0	2.636	74.54	0.25	11.75	3.16	0.01	<0.05	0.17	3.26	5.37	<0.01	<0.1	0.22	0.32
BOT 98/26/3	Bedrock	2.5	2.641	76.34	0.20	10.06	4.05	0.01	0.07	0.16	2.65	4.94	<0.01	<0.1	0.17	0.40
BOT 98/26/2	Bedrock	2.0	2.602	74.45	0.23	11.80	3.15	0.02	0.08	0.18	3.31	5.37	<0.01	<0.1	0.25	0.39
BOT 98/26/1	Bedrock	1.5	2.578	73.57	0.22	11.81	3.53	0.03	0.17	0.15	3.17	5.73	0.01	<0.1	0.19	0.44

LOI, loss on ignition

Table VII. Minor element analyses for calcrete, silcrete and granitoid-gneiss from Tswaane Quarry

Sample	Height (m)	Minor elements (ppm)													
		Ni	Cu	Zn	Ga	As	Rb	Sr	Y	Zr	Nb	Hf	Pb	Th	U
<i>Profile BOT 98/25</i>															
BOT 98/25/14	9.0	7	10	4	<1	2	5	756	9	45	2	<1	2	<1	1
BOT 98/25/13	8.5	15	16	21	5	5	55	27	2	41	3	1	4	1	4
BOT 98/25/12	8.0	13	13	19	4	3	40	75	4	33	3	<1	4	<1	3
BOT 98/25/11	7.5	8	11	17	3	4	36	75	2	25	2	<1	3	1	4
BOT 98/25/10	7.0	13	17	18	5	5	54	45	4	55	4	1	6	2	4
BOT 98/25/9	6.5	10	12	15	4	5	45	50	3	60	3	2	6	1	3
BOT 98/25/8	6.0	10	13	17	6	6	68	38	14	164	5	3	10	2	2
BOT 98/25/7	5.5	2	7	38	18	7	132	82	9	440	14	11	10	2	1
BOT 98/25/6	5.0	10	15	21	6	4	50	195	43	108	5	4	10	<1	2
BOT 98/25/5	4.5	3	6	41	18	7	134	86	9	482	15	11	10	2	1
BOT 98/25/4	4.0	2	7	53	16	7	124	83	10	394	13	9	11	2	1
BOT 98/25/3	3.5	1	6	45	21	9	141	100	13	265	10	7	16	2	1
BOT 98/25/2	3.0	4	5	52	17	8	110	87	15	364	14	9	12	1	1
<i>Profile BOT 98/26</i>															
BOT 98/26/16	9.0	5	6	20	<1	5	12	392	<1	18	2	<1	<1	<1	4
BOT 98/26/15	8.5	5	7	10	2	7	28	57	1	32	2	<1	2	<1	6
BOT 98/26/14	8.0	5	11	17	<1	7	21	235	4	29	2	2	3	<1	6
BOT 98/26/13	7.5	5	8	14	1	7	28	136	2	40	2	<1	3	<1	3
BOT 98/26/12	7.0	9	16	24	2	5	29	792	2	38	3	2	3	<1	3
BOT 98/26/11	6.5	10	13	16	3	6	36	38	1	28	2	<1	2	<1	4
BOT 98/26/10	6.0	10	17	20	7	3	61	1760	5	77	4	5	7	<1	4
BOT 98/26/9	5.5	9	17	19	4	5	52	500	14	84	3	3	9	2	2
BOT 98/26/8	5.0	10	16	12	4	9	61	56	11	124	5	3	9	1	1
BOT 98/26/7	4.5	3	5	28	17	6	139	109	9	361	14	8	13	<1	1
BOT 98/26/6	4.0	2	6	26	15	7	173	90	11	375	15	9	13	1	1
BOT 98/26/5	3.5	3	5	25	18	7	129	92	9	437	16	10	14	1	1
BOT 98/26/4	3.0	<1	4	13	13	7	128	93	10	403	16	9	15	2	1
BOT 98/26/3	2.5	<1	4	6	13	7	121	71	11	318	13	8	14	2	2
BOT 98/26/2	2.0	2	5	8	15	7	131	96	14	365	15	8	13	3	2
BOT 98/26/1	1.5	2	6	13	15	14	134	82	14	382	14	8	14	3	2

the case at Kang which is an isolated pan with its own localized catchment; silica and carbonate are likely to have been supplied radially to the pan from surface and sub-surface sources such as dust, rainwater and weathering of the Kalahari Group sediments.

There are, however, significant chemical differences between the calcretes, cal-silcretes and silcretes at both sites. Most notably, there is a strong inverse correlation between Ca and Si (Figures 6 and 7B), reflecting the inverse relationship between the percentages of silica and carbonate cements evident in thin section. An isocon comparison (Figure 8A,B) between the median calcrete and silcrete analyses (Table VIII) shows that apart from Si, the silcretes are relatively enriched in Al, Fe, Ti, K, Rb, As, Ni and Cu; by contrast, the calcretes are enriched only in Ca, Zn, Y and Sr. The gradient of the isocon drawn through Zr (i.e. assuming Zr immobility) is 1.1, almost identical to the ratio of the mean densities of calcrete and silcrete samples from Tswaane (1.08) shown in Table VI. This indicates that any volume changes associated with the calcification and silicification processes have been the same in both calcretes and silcretes; relative to each other, formation of the two duricrust types has been isovolumetric. This conclusion is consistent with the thin-section evidence which shows that both the replacement of calcrete by silica and the late-stage calcretization of the uppermost silcrete did not involve obvious volume changes.

The combined analyses from Kang and Tswaane also provide further indications of the likely environment of formation of many of the more siliceous duricrusts found at both sites. Figures 9 and 10 show that the concentrations of Al, Fe, K and Ti in all duricrusts are all very strongly correlated, with most r^2 values greater

Table VIII. Median values calculated from major and minor element XRF analyses of calcrete, silcrete, cal-silcrete and granitoid-gneiss bedrock from Kang Pan (BOT 98/29) and Tswaane Quarry (BOT 98/25 and BOT 98/26)

Location	Lithology	No. analyses	Median values for major elements (%)											Median values for minor elements (ppm)													
			SiO ₂	TiO ₂	Al ₂ O ₃	Fe ₂ O ₃ t	Mn ₃ O ₄	MgO	CaO	Na ₂ O	K ₂ O	BaO	LOI	Ni	Cu	Zn	Ga	As	Rb	Sr	Y	Zr	Nb	Hf	Pb	Th	U
BOT 98/25	Calcrete	1	9.42	0.05	0.51	0.28	0.03	0.86	48.37	0.05	0.15	0.03	39.81	7	10	4	<1	2	5	756	9	45	2	<1	2	<1	1
BOT 98/29	Calcrete	5	33.29	0.06	0.76	0.39	0.02	1.56	34.80	<0.05	0.30	0.04	28.67	6	11	100	<1	<1	9	299	9	48	1	1	4	<1	3
BOT 98/25	Cal-silcrete	1	79.07	0.13	3.04	1.54	0.03	1.63	4.98	0.08	2.23	0.03	6.26	13	13	19	4	3	40	75	4	33	3	<1	4	<1	3
BOT 98/26	Cal-silcrete	4	74.60	0.08	1.75	0.88	0.04	3.61	7.40	0.70	1.22	0.13	9.96	7	14	20	5	5	25	592	4	34	3	2	3	<1	4
BOT 98/29	Cal-silcrete	6	70.07	0.09	1.34	0.48	0.01	2.15	13.14	0.07	0.49	0.04	12.13	8	9	33	2	1	14	121	6	71	2	2	3	1	2
BOT 98/25	Silcrete	4	84.66	0.14	3.11	1.96	0.03	1.55	1.87	0.08	2.59	0.06	3.89	13	13	18	4	5	45	50	3	41	3	1	4	1	4
BOT 98/26	Silcrete	4	86.86	0.10	2.23	1.17	0.02	1.45	2.41	0.07	1.57	0.15	3.97	7	11	15	3	7	32	97	2	36	2	3	3	2	4
BOT 98/25	Basal silcrete	1	84.46	0.15	5.15	1.87	0.06	0.87	0.50	0.83	3.42	0.09	1.82	10	16	12	4	9	61	56	11	124	5	3	9	1	1
BOT 98/26	Basal silcrete	1	85.33	0.15	3.69	2.21	0.07	1.24	0.55	0.43	2.89	0.07	2.46	10	13	17	6	6	68	38	14	164	5	3	10	2	2
BOT 98/25	Bedrock	5	74.04	0.22	11.8	3.12	0.03	0.16	0.28	3.16	5.49	0.2	0.64	2	6	45	18	7	132	86	10	394	14	9	11	2	1
BOT 98/26	Altered bedrock	3	73.54	0.22	11.55	4.26	0.02	0.13	0.11	3.21	5.46	0.32	0.45	3	5	26	17	7	139	92	9	375	15	9	13	1	1
BOT 98/26	Bedrock	4	74.50	0.23	11.78	3.35	0.02	0.08	0.17	3.22	5.37	0.21	0.40	2	5	11	14	7	130	88	13	374	15	8	14	3	2

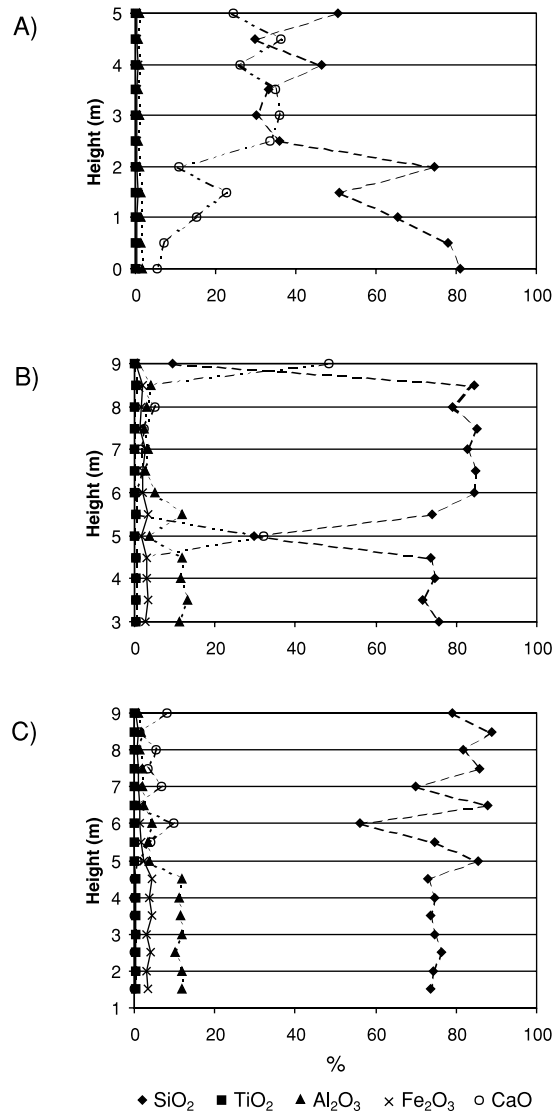


Figure 6. Results of selected XRF analyses of major elements from (A) profile BOT 98/29, (B) profile BOT 98/25, and (C) Profile BOT 98/26, showing down-profile variability in elemental concentrations

than 0.9. The highest levels of these elements are present within the silcretes from both sites (particularly those which show the strongest green colour), progressively decreasing through the cal-silcretes to the calcrites. It is most likely that these elements are present as the generally dark green, K- and Fe-rich aluminosilicate mineral glauconite, which also contains small amounts of Ti (Deer *et al.*, 1966). Glauconitic minerals constitute a continuous family with smectitic and micaceous end-members, and evolve from smectitic to micaceous through the progressive incorporation of both K and Fe (Odin and Fullagar, 1988; Kelly and Webb, 1999). Glauconite has been reported in Kalahari silcretes previously (Shaw and Nash, 1998), and its presence here is particularly supported by the very strong correlation between K and Fe (Figure 9B) within samples.

The occurrence of glauconite in the Tswane and Kang silcretes provides constraints on the geochemical environment during silicification. Glauconite occurs most commonly in shallowly buried, muddy, organic-rich sediments on the continental shelf (Odin and Fullagar 1988); it is not widely documented in terrestrial settings. In marine settings, glauconite forms under sub-oxic, partially reducing conditions, which allow ferrous iron to

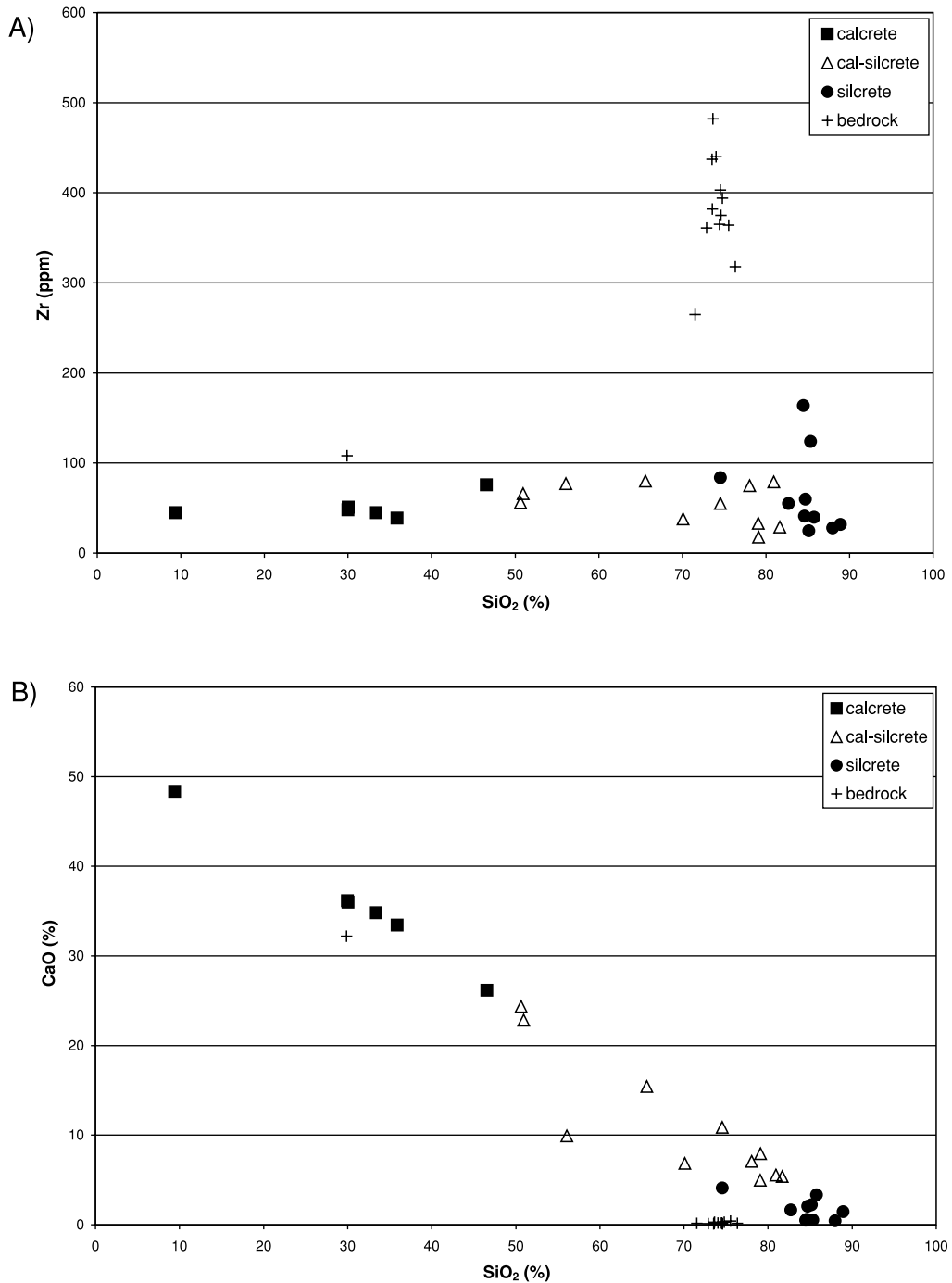


Figure 7. Relationship between (A) SiO₂ and Zr, and (B) SiO₂ and CaO concentrations in calcrete, silcrete, cal-silcrete and granitoid-gneiss bedrock samples from Kang Pan and Tswaane Quarry

be fixed in silicate structures rather than sulphides (Kelly and Webb, 1999; Kelly *et al.*, 2001). The glauconitization process occurs during very early diagenesis in a closed or isochemical system, with the constituent ions derived primarily from terrigenous clay minerals, and potassium indirectly sourced from seawater. Clearly, the glauconite in the silcreted at Kang and Tswaane formed in a very different environment. However, sub-oxic, partially

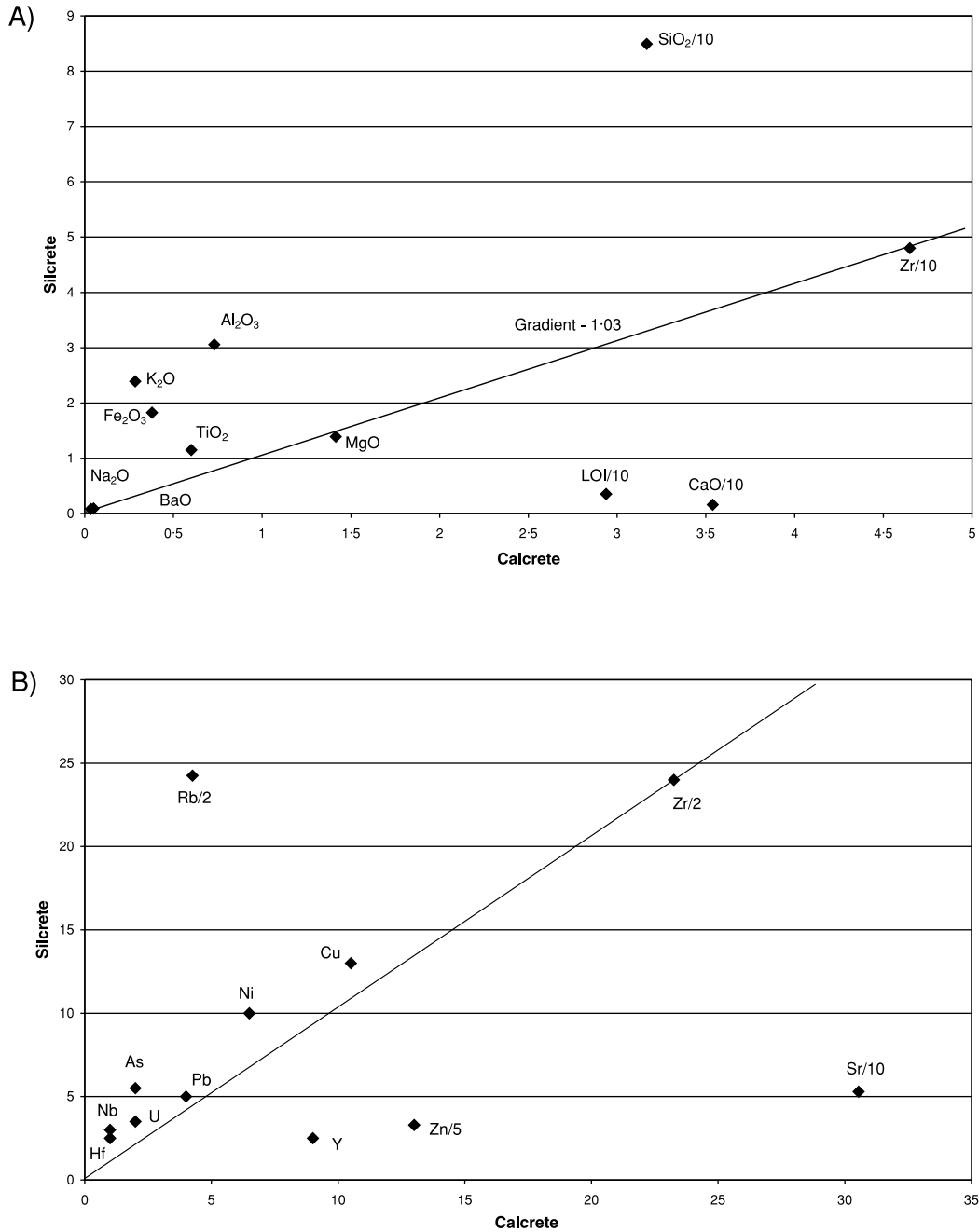


Figure 8. Isocon diagrams of median values for (A) major and (B) minor elements within calcretes and silcretes from Kang Pan and Tswaane Quarry. Numbers after oxide or element names represent scaling factors, e.g. SiO₂/10 indicates percentage value of SiO₂ divided by 10

reducing groundwaters are likely to have been present at depth at both sites where groundwater was relatively isolated from the atmosphere. It is notable that the glauconite content of the duricrusts from profile BOT 98/26 in Tswaane Quarry decreases up-profile, as shown by the progressive decrease in Al, K and Fe contents up the section (Table VI). The higher amount of glauconite at the base of the profile reflects the best conditions for glauconitization. Of the ions required for glauconite formation, Al and Ti were probably derived from

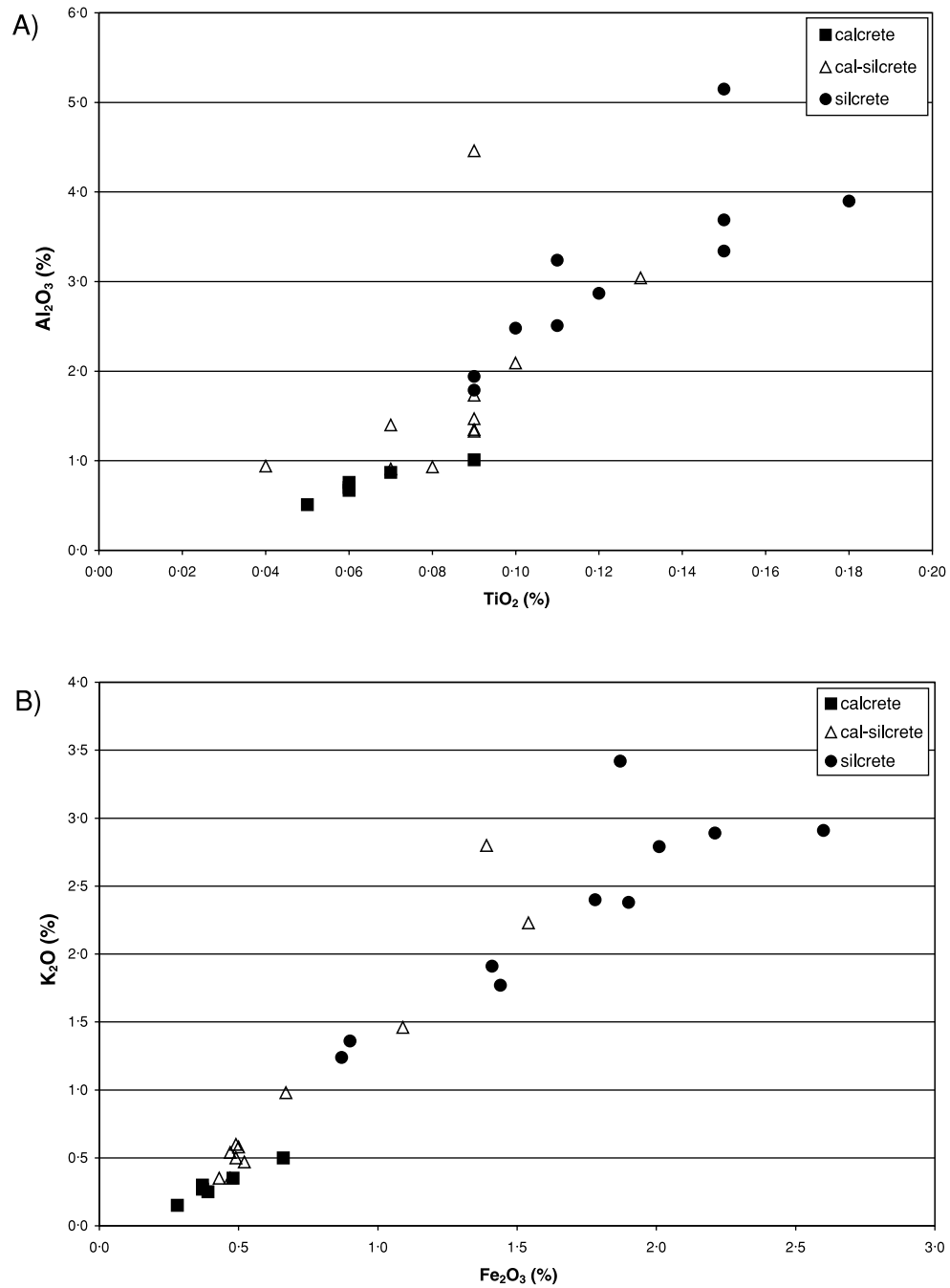


Figure 9. Relationship between (A) TiO₂ and Al₂O₃, and (B) Fe₂O₃ and K₂O concentrations in calcrete, silcrete and cal-silcrete samples from Kang Pan and Tswaane Quarry

kaolinite, which occurs in small amounts within the Kalahari Group sediments (McCarthy *et al.*, 1991), rather than from weathering of the underlying granitoid-gneiss, as there is little evidence of loss of these ions from the bedrock (discussed previously). The Al and Ti (and perhaps also the Fe) may have been leached downwards through the profile by percolating alkaline surface water, as suggested by McCarthy *et al.* (1991) for the Okavango Delta to the north.

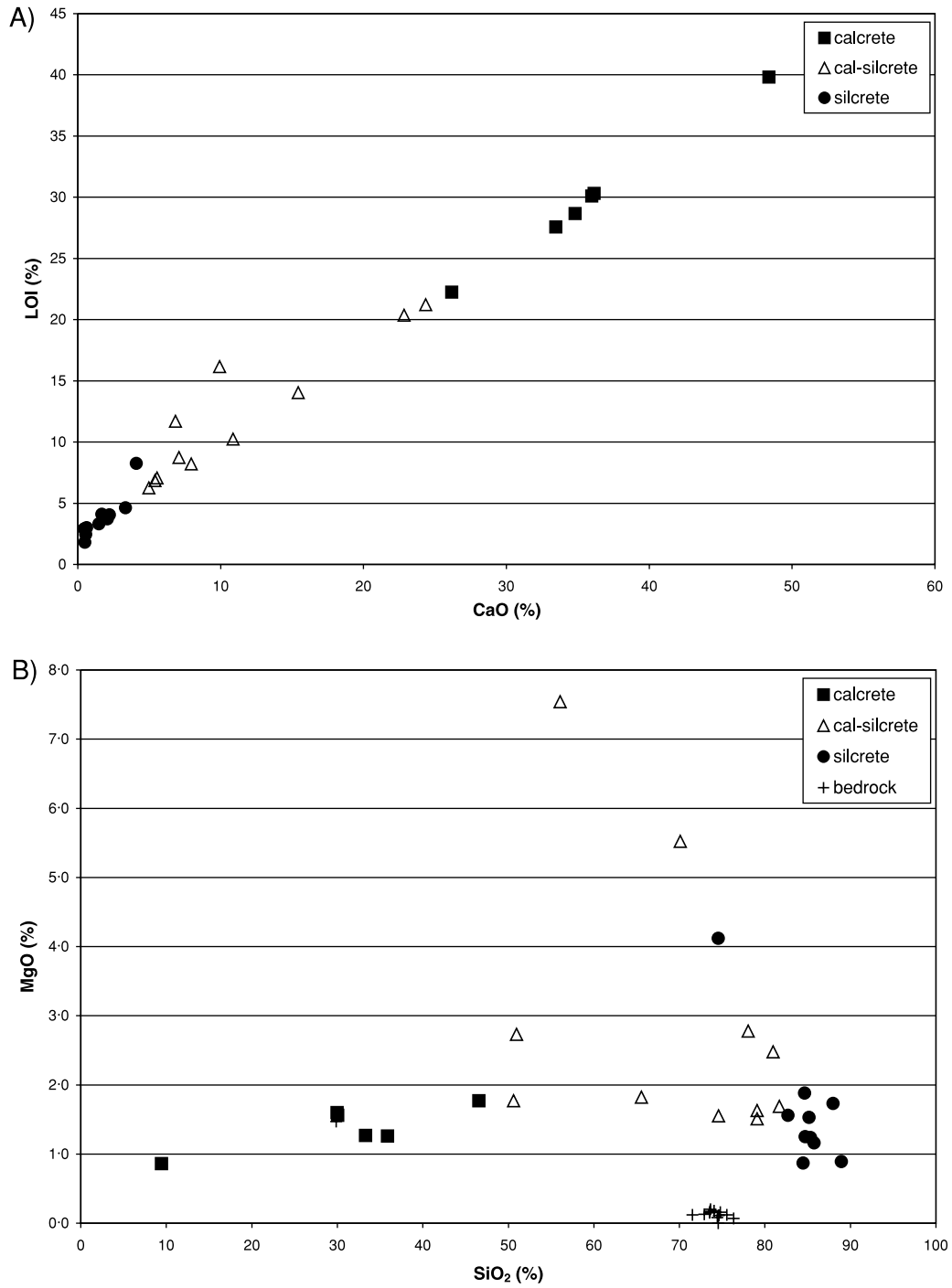


Figure 10. Relationship between (A) CaO concentrations and loss on ignition (LOI) levels in calcrete, silcrete and cal-silcrete, and (B) SiO₂ and MgO concentrations in calcrete, silcrete, cal-silcrete and granitoid-gneiss bedrock samples from Kang Pan and Tswaane Quarry

The chemical composition of the duricrusts at Kang and Tswaane also indicates that another mineral apart from glauconite is present in small amounts. Mg levels within the duricrusts are probably at least partially contained within sepiolite, a hydrous Mg silicate that is associated with silica precipitation in continental environments (Garrels and MacKenzie, 1967; Webb and Finlayson, 1987). The three samples with the highest MgO contents (>4 per cent) all have higher than expected LOI levels, as can be seen on a CaO–LOI plot (Figure 10A). LOI represents the H₂O and CO₂ content of the sample, and the collective analyses show a very strong correlation between CaO and LOI because the LOI predominantly reflects the CO₂ within the calcite in the samples. The three high-MgO samples (Figure 10B) lie above this correlation line, indicating that they have a higher LOI than would be expected from their CaO concentration; the additional LOI probably represents H₂O present in the sepiolite. On the basis of the lack of correlation between Mg and Ca, Al, Fe or K, there would appear to be little, if any, Mg in the glauconite and calcite within the duricrusts, despite the fact that Mg can substitute into the structure of these minerals. Of the other elements present within the duricrusts, Ni and Cu are at least partially present within the glauconite, because there are weak correlations between Al, Ni and Cu, and Ni and Cu are more abundant in the silcretes (Table VIII). Sr appears to be substituting for Ca within calcite, as there is a moderately good correlation between Ca and Sr, and Sr is present at higher concentrations in the calcretes.

The preceding geochemical evidence may also explain why opaque iron oxides are prevalent within cracks and voids throughout the bedrock at Tswaane, but almost completely absent from the calcrete, silcrete and intergrade duricrust samples at both locations. Whilst iron is present in all duricrust samples, the dominant iron mineral is glauconite, an aluminosilicate that formed under reducing conditions. The opaque iron oxides throughout the granitoid-gneiss precipitated under oxidizing conditions, and therefore most probably reflect a separate period of Fe mobility that predates duricrust development, rather than being concomitant with its formation.

DISCUSSION

In addition to their use in determining the likely mode of origin of the duricrusts exposed at Kang Pan and Tswaane, the macromorphological, micromorphological and geochemical data described above can also provide wider information about the development of complex cement types within silcrete–calcrete intergrade geochemical sediments. Despite originating in contrasting settings and exhibiting major differences in fabric, the suites of calcrete, silcrete and intergrade duricrusts exposed at Tswaane and Kang Pan have a number of similarities. At both sites, the duricrust assemblages have developed through the substantial silicification of a pre-existing calcrete, with silicification taking place at or below the water table. At Kang, silicification is most prevalent towards the top of the profile, probably as a result of periodic inundation of the pan surface, and at depth in association with phases of water table elevation. The partial nature of the silicification suggests that such periods or phases were not prolonged. The silicification features identified in the uppermost calcretes are very similar to those found in other Kalahari sil-calcretes (Nash and Shaw, 1998) and may, therefore, provide an important analogue for the development of intergrade cements in near-surface settings. The scenario at Kang is in marked contrast with that at Tswaane, where more extensive and pervasive silica replacement is suggestive of longer periods of groundwater silicification. On the basis of comparisons of geochemical and bulk density data, replacement at Tswaane appears to have been isovolumetric and led to the, at least partial, preservation of inherited calcrete and bedrock structures within the silcrete. In this case, silicification appears to have taken place beneath a now-fossil drainage-line, where it might be expected that a more permanently elevated water table would have existed in the past (De Vries *et al.*, 2000).

Comparison of both sites suggests, therefore, that the duration of the interaction of silica-bearing groundwater with the host calcrete is a critical determinant of the extent of any silicification that may take place. It is, however, important to note that the nature of the initial calcrete fabric may also have an important bearing upon the style and extent of silicification. In the case of Kang Pan, the precursor calcretes were highly crystalline and well-indurated and, as a result, probably relatively non-porous. As such, silicification appears to have been largely restricted to zones of higher permeability such as joints or more porous sections of the calcrete mass. This has been noted previously in studies of silicification of Kalahari calcretes (Nash and Shaw, 1998) and French limestones (Thiry and Ribet, 1999). In contrast, many of the silcrete fabrics at Tswaane are suggestive

of the replacement of largely structureless, more porous, micritic calcretes; the relatively small calcite crystal sizes in these precursor calcretes would, in theory, be more likely to permit complete replacement to take place. The potential significance of crystal size and degree of cementation is further illustrated at Kang by the style of replacement present in zones of more diffuse silicification. In these areas, silica appears to have etched around the larger sparite crystals rather than completely replacing them. It is possible that complete replacement would have taken place given more prolonged wetting, as indicated in other samples from the same profile.

The distribution of pale green (glaucoplastic) silica cements at Kang and Tswaane may also provide an indication of the contrasting environments of silicification at the two sites. At Kang, glauconite is only found in association with relatively late-stage silicification along joints. Given the environmental conditions required for glauconite formation, this silica replacement must have occurred during periods when the water table was elevated and sub-oxic, partially reducing conditions existed. The restriction of the pale green coloration to joints and joint surfaces is further suggestive that the majority of the profile was well-cemented and relatively impermeable at the time when glauconite was mobilized. In contrast, the occurrence of glauconite throughout the profile at Tswaane indicates that the majority of carbonate replacement took place beneath the water table and probably under reducing conditions. If this was the case, then the presence of green silcretes both within the quarry and exposed within the adjacent flank of the Okwa Valley (Nash *et al.*, 1994b) has major geomorphological implications as it suggests considerable incision of the Okwa since this phase of silicification. Unfortunately, it is not possible to ascertain the precise depth at which glauconitization occurred, making any estimate of the depth of incision problematic.

Finally, differences in the dominant cementing minerals within the siliceous duricrusts at both sites provide an important illustration of the potential influence of 'impurities' within pore- and groundwaters upon silicification. The silica cements within the sil-calcretes at Kang Pan are dominated by chalcedony whilst those within the more glauconitic silcretes and sil-calcretes at Tswaane are almost entirely cryptocrystalline silica. The range of silica polymorphs present within any silcrete cement depends upon a number of factors which influence the primary silica precipitation and subsequent paragenesis. Foremost amongst these are the concentration of SiO_2 in solution, and the temperature, pressure and environmental pH and Eh of the solution. However, dissolved constituents such as Fe^{3+} , UO_2^+ , Mg^{2+} , Ca^{2+} , Na^{2+} and F, may also react with the silica within a solution to form complexes (e.g. Chadwick *et al.*, 1989), whilst salts such as NaCl may change the solvent properties of the solution (e.g. Dove and Rimstidt, 1994). As such, the presence of iron associated with the formation of the K-Fe aluminosilicate glauconite at Tswaane may have restricted the development of more fibrous cements such as chalcedony and favoured the precipitation of cryptocrystalline silica. The precipitation of chalcedonic void-fills during later stages of the evolution of the profiles further supports this suggestion.

CONCLUSIONS

Despite a wealth of studies of silcretes and calcretes in the Kalahari and elsewhere, this is the first time that an investigation of the petrology and chemistry of relatively 'fresh' unweathered calcrete-silcrete intergrade duricrust profiles has been undertaken. Complex suites of non-pedogenic duricrusts exposed in aggregate pits at two sites in the central Kalahari, Kang Pan and Tswaane, have been described in terms of their micromorphological and geochemical properties. Duricrust development at both locations was strongly influenced by the position of the water table, itself related to the geomorphological context of each site. The duricrust exposure at Kang Pan consists of a massive, well-cemented crystalline alpha-fabric calcrete, developed within Kalahari Group sands, which has been extensively silicified in its upper and, especially, lower sections. Late-stage voids-fills indicate the continuing circulation of silica and carbonate-rich porewaters following this phase of silicification. The distribution of silica cements at this site appears to have been determined by fluctuations of the water table in lower sections and periodic inundation by surface waters in uppermost parts of the profile. The specific location and style of silicification within the profile was also influenced by factors such as the degree of cementation and permeability of the calcrete. In contrast, the quarry at Tswaane reveals a duricrust suite with a more complex history. At this site, a pre-existing calcrete has been isovolumetrically replaced by a glauconite-rich groundwater silcrete which has, in turn, been partly replaced by a later phase of calcification associated with the development of a near-surface non-pedogenic calcrete. The development of both the silcrete and secondary calcrete cements

was closely controlled by porosity and permeability variations within the duricrust profile. Formation was also closely linked to water table fluctuations associated with incision of the adjacent Okwa Valley, with the silicification and calcification occurring below the water table prior to a major phase of downcutting.

Geochemical evidence indicates that, despite being developed on top of granitoid-gneiss, the profile at Tswaane contains little bedrock-derived material either as part of the original host sediment or within the constituents of the calcareous and siliceous cements. Furthermore, the bedrock does not exhibit a chemical weathering profile, despite evidence of superficial alteration. This would suggest that the majority of the silica and carbonate species within the duricrust suite were derived externally as opposed to being moved vertically from the underlying bedrock. Given the similarity in chemistry between the duricrusts at both Kang and Tswaane it is likely that the cements within the intergrade duricrusts at Kang were also derived non-locally. Overall, the combination of micromorphological and geochemical approaches used in this study clearly demonstrates the potential of detailed sampling and analysis for determining the environment and mechanisms of duricrust formation. It also serves to reinforce the significance of topographic depressions (pans and valleys) upon the formation of calcrete, silcrete and calcrete–silcrete intergrade duricrusts within the Kalahari.

ACKNOWLEDGEMENTS

This research was funded by the universities of Brighton and Leicester, with additional support for XRF analyses provided by the Research and Publications Fund of the British Geomorphological Research Group. XRF analyses were undertaken at the Analytical Geochemistry Laboratories of the British Geological Survey, Keyworth, UK. The authors would like to thank John Bollard and David Harris (University of Brighton) for thin-section and sample preparation.

REFERENCES

- Aldiss DT, Carney, JN. 1992. The geology and regional correlation of the Proterozoic Okwa Inlier, western Botswana. *Precambrian Research* **56**: 255–274.
- Arakel AV. 1986. Evolution of calcrete in palaeo-drainages of the Lake Napperby area, central Australia. *Palaeogeography, Palaeoclimatology, Palaeoecology* **54**: 283–303.
- Arakel AV, Jacobson G, Salehi M, Hill CM. 1989. Silicification of calcrete in palaeodrainage basins of the Australian arid zone. *Australian Journal of Earth Sciences* **36**: 73–89.
- Aristarain LF. 1970. Chemical analyses of caliche profiles from High Plains, New Mexico. *Journal of Geology* **78**: 201–212.
- Balan E, Neuville DR, Trocellier P, Fritsch E, Muller JP, Calas G. 2001. Metamictization and chemical durability of detrital zircon. *American Mineralogist* **86**: 1025–1033.
- Brown CN. 1956. The origin of caliche in the northwestern Llano Estacado, Texas. *Journal of Geology* **64**: 1–15.
- Butt CRM. 1985. Granite weathering and silcrete formation on the Yilgarn Block, Western Australia. *Australian Journal of Earth Sciences* **32**: 415–432.
- Chadwick OA, Hendricks DM, Nettleton WD. 1987. Silica in duric soils. A depositional model. *Soil Science Society of America Journal* **51**: 975–982.
- Chadwick OA, Hendricks DM, Nettleton WD. 1989. Silicification of Holocene soils in Northern Monitor Valley, Nevada. *Soil Science Society of America Journal* **53**: 158–164.
- De Vries JJ, Selaolo ET, Beekman HE. 2000. Groundwater recharge in the Kalahari, with reference to paleo-hydrologic conditions. *Journal of Hydrology* **238**: 110–123.
- Deer WA, Howie RA, Zussman J. 1966. *An Introduction to the Rock-forming Minerals*. Longman: London.
- Dove PM, Rimstidt JD. 1994. Silica-water interactions. In *Silica: Physical Behaviour, Geochemistry and Materials Applications*, Heaney PJ, Prewitt CT, Gibbs GV (eds). Reviews in Mineralogy 29. Mineralogical Society of America: Washington; 259–308.
- Folk RL, Pittman JS. 1971. Length-slow chalcedony: a new testament for vanished evaporites. *Journal of Sedimentary Petrology* **41**: 1045–1058.
- Garrells RM, MacKenzie FT. 1967. Origin of the chemical composition of some springs and lakes: equilibrium concepts in natural water systems. *American Chemical Society Advances in Chemistry Series* **67**: 222–242.
- Grant JA. 1986. The isocon diagram – a simple solution to Gresens' Equation for metasomatic alteration. *Economic Geology* **81**: 1976–1982.
- Gresens RL. 1967. Composition-volume relationships of metasomatism. *Chemical Geology* **2**: 47–55.
- Hay RL, Wiggins B. 1980. Pellets, ooids, sepiolite and silica in three calcretes of the southwestern United States. *Sedimentology* **27**: 559–576.
- Hutton JT, Twidale CR, Milnes AR. 1978. Characteristics and origin of some Australian silcretes. In *Silcrete in Australia*, Langford-Smith T (ed.). Department of Geography, University of New England: Armidale, New South Wales; 19–39.
- Kelly JC, Webb JA. 1999. The genesis of glaucony in the Oligo-Miocene Torquay Group, southeastern Australia: petrographic and geochemical evidence. *Sedimentary Geology* **125**: 99–114.
- Kelly JC, Webb JA, Maas R. 2001. Isotopic constraints on the genesis and age of autochthonous glaucony in the Oligo-Miocene Torquay Group, southeastern Australia. *Sedimentology* **48**: 325–328.

- King LC. 1967. *The Morphology of the Earth* (second edition). Oliver and Boyd, Edinburgh.
- Mallick DIJ, Habgood F, Skinner AC. 1981. *A Geological Interpretation of Landsat Imagery and Air Photography of Botswana*. Institute of Geological Sciences, Overseas Geology and Mineral Resources 56. HMSO: London.
- McCarthy TS, McIver JR, Verhagen BT. 1991. Groundwater evolution, chemical sedimentation and carbonate brine formation on an island in the Okavango Delta swamp, Botswana. *Applied Geochemistry* **6**: 577–595.
- Nash DJ, McLaren SJ. 2003. Kalahari valley calcretes: their nature, origins and environmental significance. *Quaternary International* **111**: 3–22.
- Nash DJ, Shaw PA. 1998. Silica and carbonate relationships in silcrete-calcrete intergrade duricrusts from the Kalahari of Botswana and Namibia. *Journal of African Earth Sciences* **27**: 11–25.
- Nash DJ, Shaw PA, Thomas DSG. 1994a. Duricrust development and valley evolution: process-landform links in the Kalahari. *Earth Surface Processes and Landforms* **19**: 299–317.
- Nash DJ, Thomas DSG, Shaw PA. 1994b. Siliceous duricrusts as palaeoclimatic indicators: evidence from the Kalahari Desert of Botswana. *Palaeogeography, Palaeoclimatology, Palaeoecology* **112**: 279–295.
- Odin GS, Fullagar PD. 1988. The geological significance of the glaucony facies. In *Green Marine Clays*, Odin GS (ed.). Elsevier: Rotterdam; 295–332.
- Price WA. 1933. The Reynosa problem of south Texas and the origin of caliche. *Bulletin of the Association of Petroleum Geologists* **17**: 488–522.
- Reeves CC. 1970. Origin, classification and geologic history of caliche. *Journal of Geology* **78**: 86–95.
- Reeves CC. 1976. *Caliche: Origin, Classification, Morphology and Uses*. Estacado Books: Lubbock, Texas, USA.
- Ringrose S, Kamunzo AB, Vink BW, Matheson W, Downey WS. 2002. Origin and palaeo-environments of calcareous sediments in the Moshaweng Dry Valley, Southeast Botswana. *Earth Surface Processes and Landforms* **27**: 591–611.
- Shaw PA, De Vries, JJ. 1988. Duricrust, groundwater and valley development in the Kalahari of south-east Botswana. *Journal of Arid Environments* **14**: 245–254.
- Shaw PA, Nash DJ. 1998. Dual mechanisms for the formation of fluvial silcretes in the distal reaches of the Okavango Delta Fan, Botswana. *Earth Surface Processes and Landforms* **23**: 705–714.
- Sidwell R. 1943. Caliche deposits of the southern High Plains, Texas. *American Journal of Science* **241**: 257–261.
- Smith BJ, Whalley WB. 1982. Observations on the composition and mineralogy of an Algerian duricrust complex. *Geoderma* **28**: 285–311.
- South African Committee for Stratigraphy (SACS). 1980. *Stratigraphy of South Africa Part 1. Lithostratigraphy of the Republic of South Africa, South West Africa/Namibia, and the Republics of Bophuthatswana, Transkei and Venda*. Handbook of the Geological Survey of South Africa 8. Geological Survey of South Africa: Pretoria.
- Summerfield MA. 1982. Distribution, nature and genesis of silcrete in arid and semi-arid southern Africa. *Catena, Supplement* **1**: 37–65.
- Summerfield MA. 1983a. Silcrete. In *Chemical Sediments and Geomorphology*, Goudie AS, Pye K (eds). Academic Press: London; 59–91.
- Summerfield MA. 1983b. Petrography and diagenesis of silcrete from the Kalahari Basin and Cape Coastal Zone, southern Africa. *Journal of Sedimentary Petrology* **53**: 895–909.
- Summerfield MA. 1983c. Geochemistry of weathering profile silcretes, southern Cape Province, South Africa. In *Residual Deposits: Surface Related Weathering Processes and Materials*, Wilson RCL (ed.). Special Publication 11. Geological Society: London; 167–178.
- Summerfield MA. 1984. Isovolumetric weathering and silcrete formation, southern Cape Province, South Africa. *Earth Surface Processes and Landforms* **9**: 135–141.
- Swineford A, Franks PC. 1959. Opal in the Ogallala Formation in Kansas. *Society of Economic Palaeontologists and Mineralogists Special Publication* **7**: 111–120.
- Thiry M, Ben Brahim M. 1990. Silicifications pédogénétiques dans les dépôts hamadiens du piémont de Boudenib (Maroc). *Geodinamica Acta* **4**: 237–251.
- Thiry M, Ben Brahim M. 1997. Ground-water silicifications in the calcareous facies of the Tertiary piedmont deposits of the Atlas Mountain (Hamada du Guir, Morocco). *Geodinamica Acta* **10**: 12–29.
- Thiry M, Ribet I. 1999. Groundwater silicification in Paris Basin limestones: fabrics, mechanisms, and modelling. *Journal of Sedimentary Research* **69**: 171–183.
- Thomas DSG, Shaw PA. 1991. *The Kalahari Environment*. Cambridge University Press: Cambridge.
- Thornber MR. 1992. The chemical mobility and transport of elements in the weathering environment. In *Regolith Exploration Geochemistry in Tropical and Subtropical Terrains*, Butt CRM, Zeegers H. (eds). Handbook of Exploration Geochemistry 4. Elsevier: Amsterdam; 79–96.
- Vaniman DT, Chipera SJ, Bish DL. 1994. Pedogenesis of siliceous calcretes at Yucca Mountain, Nevada. *Geoderma* **63**: 1–17.
- Watts NL. 1980. Quaternary pedogenic calcretes from the Kalahari (southern Africa), mineralogy, genesis, and diagenesis. *Sedimentology* **27**: 661–686.
- Watts SH. 1978. A petrographic study of silcrete from inland Australia. *Journal of Sedimentary Petrology* **48**: 987–994.
- Webb JA, Finlayson BL. 1987. Incorporation of Al, Mg and water in opal-A: evidence from speleothems. *American Mineralogist* **72**: 1204–1210.
- Webb JA, Golding SD. 1998. Geochemical mass-balance and oxygen-isotope constraints on silcrete formation and its paleoclimatic implications in Southern Australia. *Journal of Sedimentary Research* **68**: 981–993.
- Wright EP. 1978. Geological studies in the northern Kalahari. *Geographical Journal* **144**: 235–250.
- Wright VP, Tucker ME. 1991. *Calcretes*. Blackwell: London.